

Multisource Investigation, Mapping and Analysis of the Tectonic Paleozoic Structures and their Surface Expressions in Ghadamis Basin and the Al Qarqaf Arch, using GIS, Satellite Remote Sensing, Aeromagnetic, Seismic Cross Sections and DEM

Dr. Mahmoud Ali Benissa

Libyan Petroleum Institute, exploration Department, P.O. Box 6431 Tripoli-Libya

Abstract: *The main goal is to combining and merging of different satellite remote sensing images and geological-geophysics data, (surface and subsurface characteristics of Ghadamis basin). A major analysis of the Earth Observation Data (EOD) was also undertaken in order to better understand the structural geology in the region with a view to using them as direct analogues to assist in the interpretation of the equivalent horizons in the subsurface data. The merging of multiple data sets has given a better understanding of the tectonic process, surface and subsurface structural styles resulting from the various deformational phases. This study is based on new work carried out on several different types of satellite imagery at different resolutions; these data were combined with the SRTM DEM (90m. ground resolution) to give better visualisation of the structures and interpretation. This study provides an overview of the structural framework and overall architecture of the Ghadamis Basin and Al Qarqaf Arch, on a regional scale using remote sensing, aeromagnetic maps and seismic sections. The main objective in this study is to applying the new techniques and methodology for mapping and analysing the surface expressions of geological structures using remote sensing images and GIS for merging. The remote sensing data set comprises digital enhancement and interpretation of SPOT XS, Landsat TM 5&7 and ERS-2 images, Goggle Earth viewer, and ASTER GDEM to map surface structures (Table 1). A variety of regional geoscience datasets from Ghadamis Basin have been co-registered and analysed using a geographic information system (GIS). The datasets include bedrock and surficial geological maps and airborne geophysical survey data. A number of line features, including structural lineaments, fold axes and formation contacts, have also been interpreted. The GIS uses a quad tree structure, ideally suited to a mixture of polygonal-thematic (e.g., geological maps) and continuous "grey-scale" (e.g., remote sensing, airborne geophysics) raster images. This study is based on the use of satellite remote sensing and GIS techniques, for refinement of the exploration models for the area and selection of areas for further more detailed investigations. More especially it will explore advanced satellite image processing software such as ER Mapper and ESRI ArcGIS. I shall make use of new acquired satellite data and advanced processing techniques and I shall tend, in the frame of GIS, to answer questions relating to exploration problems. In particular, recent satellite imagery, especially when digitally reprocessed, can prove to be a practical way of rapidly surveying a large amount of land and can help define new prospective areas with rejuvenated concepts.*

Keywords: Ghadamis Basin, Al Qarqaf Arch, Paleozoic, GIS, Remote sensing, Aeromagnetic, seismic cross sections and DEM

1. Objectives

The main goal and objective of this study is directly related to the interpretation of the structure geology issue of the influence on hydrocarbon explorations. With this in mind, answers to the following research questions were sought:

- 1) What are the Palaeozoic arch configurations? , what is the relation to adjacent sedimentary basins to hydrocarbon accumulations?
- 2) What is the surface structural and expressions in the Ghadamis Basin?, and what is the significance for hydrocarbon explorations?

The using of advanced approach in this study (Ghadamis Basin and Al Qarqaf Arch), will be used to combine the data and information leading to structural models.

The second objective is essentially to present and assess tools for a multisource investigation, mapping and analysis of the tectonic Paleozoic structures and their surface expressions in Ghadamis Basin and the Al Qarqaf Arch, using GIS, satellite remote sensing, aeromagnetic, seismic

cross sections and DEM. (Benissa, M.A. and J. Chorowicz, 2016).

We will focus on analysing the influence of the structural framework of the Paleozoic rocks in Al Qarqaf Arch, the Ghadamis Basin and adjacent areas and its implication for hydrocarbon accumulations in the region. The Geological interpretation model will be divided into two parts:

- 1) Analysis of the tectonics of the Palaeozoic Basement in the Al Qarqaf Arch (Benissa, M.A. ,J.Chorowicz, 2016).
- 2) Analysis of drainage pattern and depressions as sinkholes in the Meso-Cenozoic cover rocks of the Ghadamis Basin (Scientific paper under correction, revision and printing).

By using new acquisition methods and advanced processing techniques will answer many questions relating to the exploration problems, can be done partly by using remote sensing and GIS. All of these questions (problematics) will be discussed and answered in this paper.

To achieve the goals to the aforementioned study questions, all available geological data, geophysical (Seismic,

Aeromagnetic and Gravity) data, remote sensing images, oil and gas wells, and oil field data have been used.

2. Introduction

Commercial remote sensing (for non-weather applications) from space largely began with the launch of Landsat-1 in 1972. Since that time, commercial remote sensing satellites have been launched by many countries, but the primary ones are the USA, France, Canada, Europe, and Japan. Recently, Russian groups have begun marketing data from their satellites, as well.

The vast majority of all remote sensing is based on the electromagnetic spectrum (EMS), and thus includes such sensors as: photographic cameras; radar; lasers; infrared scanners, radiometers and imagers; spectrometers; microwave radiometers; and multispectral scanners (MSS). It is not unusual to have multistage, multi-sensor image interpretation; the geologist may start with a small-scale (e.g., 1:250,000 to 1:1,000,000) satellite image, then move to a larger scale high-altitude aerial photographs 1:40,000 and then to a larger scale traditional air photo, followed by other remote-sensing products (e.g., gravity, seismic surveys; radar) as are appropriate for the information being sought.

The importance of this use of multiple sensors is that features such as lineaments may appear differently on images from different sensors or not at all; the maximum amount of information, and the closest approximation to reality, is obtained by integrating data sets (Barringer, 1970) The remote sensing techniques most often used in geology are aerial photography and multispectral scanning, the latter in the form of satellite data such as Landsat images (MSS and Thematic Mapper, TM), (Barringer, 1970). One major benefit of satellite imagery, the vast amount of data, is also a major problem, which is increasingly dealt with by utilizing digital image processing, since all non-camera images is initially digital data.

Data

Studying data base constitution has included data gathering, screening and organization; it can be incorporated in a Company data base. The format of the data base has the international standard and can be updated when new data is acquired.(Table 1), summarize the data used in the study.

Multiple data set integration and/or merging for structural interpretation of the Ghadamis basin using ArcGIS Software. It demonstrates the integration of remote sensing data as well as subsurface information data in order to obtain

a better and more comprehensive of the geology of multi-layers from surface to the basement. A digital database was constructed for the data collected and integrated in different parts of the study.

In general, three main different types of satellite remote sensing data have been used in different parts of the study. About 12 Landsat ETM7 images plus one scene of Mosaic, 16 Landsat TM5 images plus one Mosaic, 10 Spot 4 XS images, 9 Spot 5 XS images (North-west Libya) and 12 Radar ERS-2 images (Table 1). These data were combined with the SRTM DEM (90 m. ground resolution) to give better visualization of the structures and interpretation, were digitally enhanced and used for mapping structural features, lineament analysis and stratigraphy of the area of study. Landsat TM and ETM, Spot XS and Radar ERS-2 were merged for mapping surface structures, partly covered by sand sheets, in the central part of Al Qarqaf Arch. Landsat TM 5 and ETM 7 images were also used to map fault patterns in the area of Al Qarqaf Arch.

Aeromagnetic data derived from a compilation of the African continent, and compiled at 1 Km., terrain elevation (AMMP, 1992). Some of selected Seismic sections were used in GhadamisBasin for mapping the fault and fold patterns. Unfortunately, no good seismic sections were made available for the GhadamisBasin.

The following data was also used during the interpretation:

- 1:250,000 scales published geological maps. The 13Coloured Geological maps as a raster and analog with Scale: 1: 250,000, One Geological map as a raster and analog of NW Libya with Scale: 1: 1000, 000and 12 Geological maps as a raster and analog with Scale: 1:50,000, were scanned and georeferenced to the satellite imagery.
- Various published reports on the geology and tectonics of the area (see Reference List).
- 1:500,000 scale seismic base map and representative interpreted seismic lines provided by LPI. The map was scanned and referenced to the satellite imagery and used for locating seismic lines, regional subsurface basement related structural features, oil wells and producing oil fields.
- 1:500,000 regional Potential Fields data provided by LPI including digital files of processed gravity and magnetic together with related residual and derivative maps. These were used for comparing the surface structure, particularly the position and continuation of surface faults into the basement.

Table 1: Summary of data types, formats, numbers, analysis products, specifications and analysis of remote sensing images used in Ghadamis Basin and Al Qarqaf Arch.

Data Type (Satellite\Sensor)	Numbers Of Scenes	Path/Row Or Orbit/Fram	BAND Combination and \ or Acquisition Date	Data Type	Final Analysis and Production
Landsat ETM7	12 plus one (Mosaic)	187\37-40 at 03.04.1987 188\37-40 at 20.01.1987 189\37-40 at 04.06.1987	7,4,2 & 8 (RGB & I)	Raster Cell size 15m. (Pixel size of mosaic: resampled to 60m).	Structural and lithological mapping, lineaments analysis

Landsat TM5	16 plus one (Mosaic)	N32\20-35 N33\20-30 N34\20-30	7,4,2 (RGB)	Raster Cell size 30m. (Pixel size of mosaic: resampled to 60m).	
SPOT XS 4	10	73\291,293 74\291-293 75\291-295	1,2,3 (G R IR)	Raster 20 meters resolution	
SPOT XS 5	09	310-541 357-541, 596,651 405-596 452-541,596 500-541,596	1,2,3 (G R IR)	Raster 5 meters resolution	
DEM (Digital Elevation Model)	1 scene	Entire area (28-32 N and 09 -14 E)	1999	Raster 900 m.	
RADAR ERS-2 Synthetic Aperture Radar (SAR)	12 Scene	28361 3015 26128 3033 28361 3033 26128 3015 14950 549 14950 567 15194 549 15194 567 2979 26128 2979 27402 3051 17611 26128 2997	Lat:29.386, Long: 14.011 Lat:28.500, Long: 13.061 Lat:28.494, Long: 13.796 Lat:29.392, Long: 13.275 Lat:27.815, Long: 14.187 Lat:28.706, Long: 13.976 Lat:27.382, Long: 13.427 Lat:28.721, Long: 13.216 Lat:31.179, Long: 13.690 Lat:31.166, Long: 12.980 Lat:27.598, Long: 12.850 Lat:30.284, Long: 13.491	Raster provides the textural information 12.5 m. resolution C- Wavelength (.056666 cm.)	
Geophysical Data	Gravity	1 scene	Entire area (28-32 N and 09 -14 E)	(1 and 8 Km. resolution)	Raster
	Aeromagnetic	1 scene	Entire area (28-32 N and 09 -14 E)	(1 and 8 Km. resolution)	Raster
	Seismic Tectonic displacement map Seismic sections.	3 Regional seismic section in North , Central and south Ghadamis Basin	Entire area (28-32 N and 09 -14 E)	Selected Cross-Section A, B and C	Raster
Geological Maps	13	Entire area (28-32 N and 09 -14 E)	Scale:, 1: 50,000, 1: 250 000 and 1: 1000 000	Raster and Analog	Integration
Goggle Earth viewer	-----	-----	-----	-----	Analysis-Drawing
EnviSat ASTER GDEM	-----	-----	-----	-----	Analysis-Drawing

Data analysis systems were used to process and enhance the data: ER-Mapper®, Global Mapper®, Blackart®, Photomod Radar Viewer®, surfer®, 3dem®, ArcMap®, MrSID Viewer®, SRTM®, GEOTIFF®, ERDAS Imagine® and Google Earth Viewer® were used for remote sensing image processing and analysis; and ArcGIS software® was used for constructing different subsurface and surface maps, Georient software® was used for constructing the plots from the field measurements of dip, strike and striations of faults. Adobe Photoshop®, Adobe Illustrator® and Freehand® was used for drafting the maps and sections.

The LPI (Libyan Petroleum Institute) is considered to be the principal source of information. A secondary source would be the companies operating in Libya. Some of the data are already in a digital form, the other data exist only in hard copy and we made the digitising and geo-rectified.

3. Various Types of Data

3.1 Aeromagnetic Data

Geophysical methods that penetrate into the Earth's surface are often used for mineral and petroleum exploration, and first used for geologic work by USGS in 1943.

The aeromagnetic data used in the study is part of the African Magnetic Mapping Project (AMMP, 1992). It is a digital 1km. X 1km. grid of total field anomaly upward continued to 1km above topography (Figure 1).

In magnetic properties the basement rocks can have large contrasts, resulting in high amplitude magnetic anomalies. When the basement rocks are shallow, the strong, short wave length anomalies they produce can obscure any weaker anomalies of similar wavelengths produced by sedimentary rocks (Figure 1). When the basement rocks are deep, their anomalies become broader, and therefore can be separated from the more localised anomalies of the shallow sedimentary rocks by appropriate wavelength filtering.

Young volcanic units tend to produce strong magnetic anomalies at all wavelengths, which obscure anomalies from

underlying sedimentary units (Jeffrey, et. al., 1998).

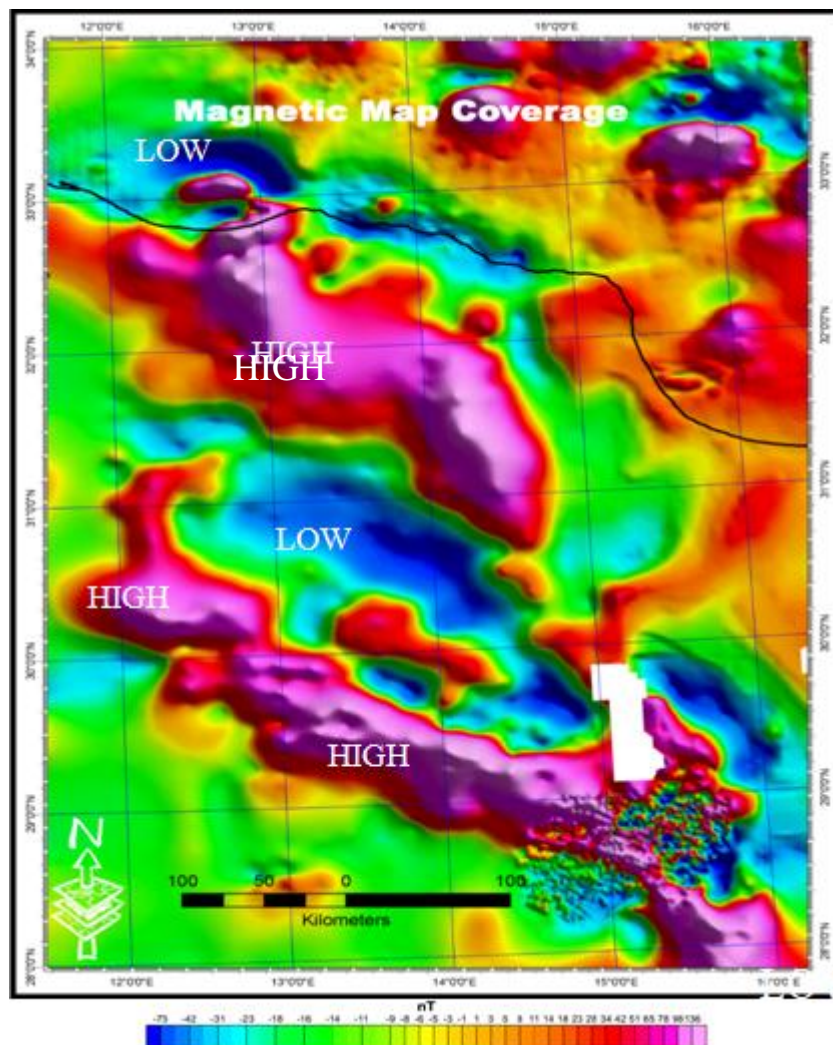


Figure 1: Second vertical derivative map of the total intensity aeromagnetic

The aeromagnetic image of the area was filtered to remove any frequency noise that may influence the derivative images. From the total intensity magnetic anomalies (Figure 1), a reduction to the pole anomaly map was made. This map clearly shows a series of magnetic highs and lows in the area. Several processing were applied to this image, including sun shading and second vertical derivative. (Figure 1) shows the second vertical derivative of the magnetic data.

3.2 Digital Terrain Model Data (DTMD) \ Elevation Model Data (EMD)

Digital Terrain Model with 1km. (Figure 2a and 2b)), resolution was used to describe the topography of the area (Figure 2a and 2b). A Digital Elevation Model (SRTM-DEM) consists of a sampled array of elevations for ground positions that are normally at regularly spaced intervals. The one degree DEM (3x3 arc-second data spacing) provides coverage in 1°/1° blocks for the area of study.

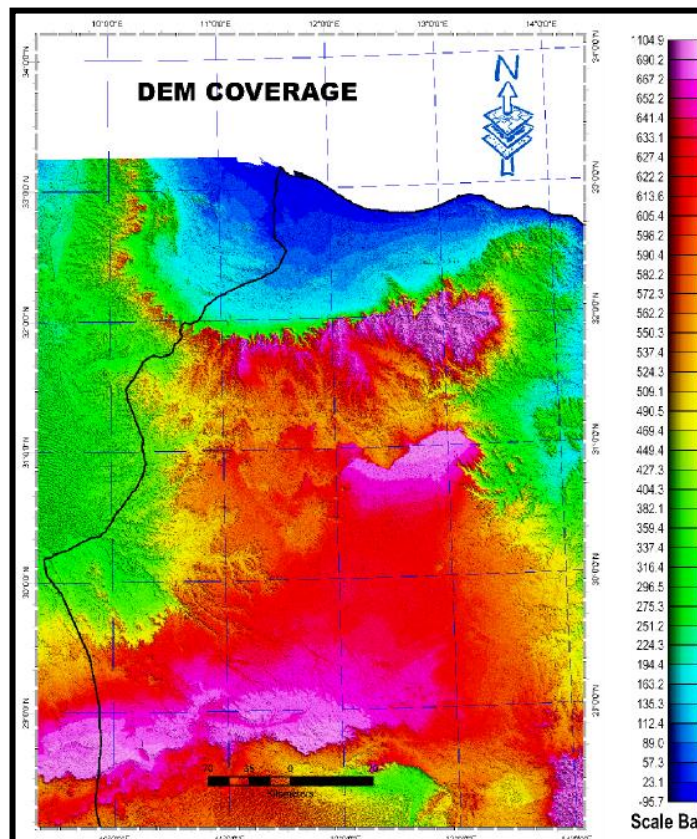


Figure2 (a): DEM of the study area, (data from USGS 1km), colored and shaded from NE

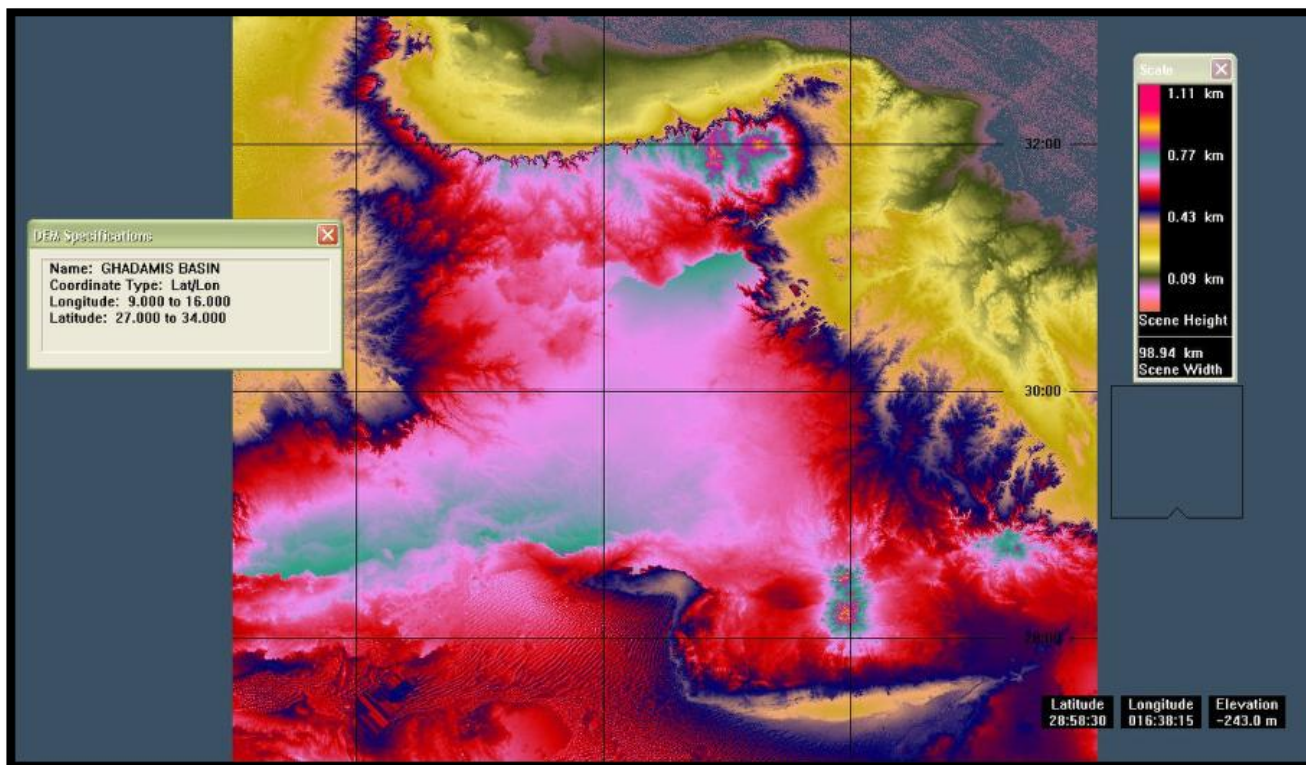


Figure2 (b): DEM of the study area, (data from USGS 1km), colored and shaded from NE

3.3 Drilling wells and field database

Comparison of the structural interpretation with the drilling wells and field database revealed a large number of surface features that resemble structures with proved hydrocarbon accumulations (Figure 3). When the newly interpreted

features (leads) are compared with hydrocarbon play maps, known fields and well locations, many apparently untested exploration targets are immediately apparent. The leads are primarily structural traps with a related surface expression as interpreted from the data used. A GIS package has been constructed for the area of structural and other geologic data.

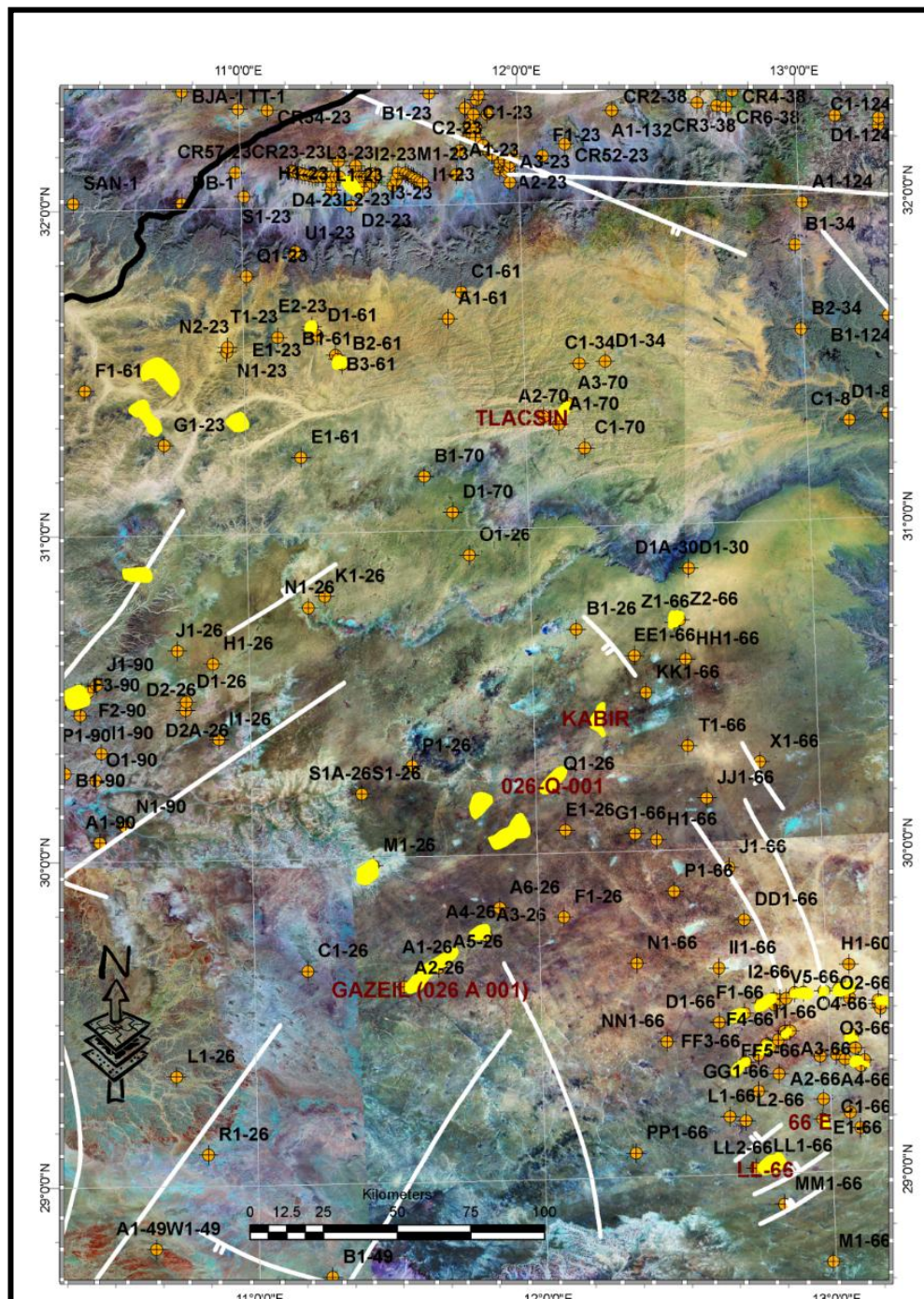


Figure 3: Map showing the structural interpretation with the drilling wells and fields database.

Remote sensing associated to structural analysis in the field is a powerful tool for tectonic studies. Satellite imagery allows locate and precisely map the faults (Chorowicz et al., 1983; Chorowicz et al., 1994; Chorowicz & Deroin, 2003) in the frame of a Geographic Information System (GIS).

Our approach depends on the study objective, which is to determine the deformation style at regional scale for the Palaeozoic time. In the field, it is practicable to perform structural analysis of faults, i.e., local measurements of gouge slicken-sides. GIS and GPS (Ground Positioning System) permit to carry out field structural analysis at the locations previously chosen by remote sensing.

On satellite imagery, it is possible to map the overall pattern of deformation over a large area, from chosen locations, in

order to learn about fault apparent movements. Fault mechanisms can then be assessed by this mapping and by sufficient sites of measurements of local movements during fieldwork. Brittle deformation at regional scale principally corresponds to movements along the major faults. Minor faults account for a minor part of the regional deformation. The fault movements need to be assessed by fault structural analysis in the field.

Accessible interesting locations are determined from our GIS dataset, and their geographic coordinates determined. Using GPS it is then possible in the field to reach these locations and walk along the fault traces for structural analysis.

We measured the dip and strike of fault plane and sense of movement at each fault we could get to, basing our observations mainly on the striations and movement indicators such as Riedel features, striating elements, quartz steps, displacement of remarkable layers. Instead of using inversion techniques that are frequently dedicated to determine the local stress components from strain, and afterward deduce the regional deformation from considering the stress field, we directly focused on the movement at each mapped fault, with special interest in the horizontal component of movement.

In the field, the main fault plane sometimes can be observed directly, and its striations measured. In some sites, the main fault plane is not determined with certainty, but faults that are paralleling each other in a given site are supposed to have the same mechanism, and consequently the movement along the main fault is chosen to be that of minor planes that have the same strike and dip.

3.4 Remote Sensing Data

Remote Sensing activities conducted by the petroleum exploration companies in Libya were restricted to aerial photograph interpretations during the 1960's. Oil exploration companies are presently using remote sensing as a strategic tool to achieve cost benefits and competitive

advantage. The satellite remote sensing data are becoming a top priority in the search for the future natural resources to be found in the remaining prospective areas of the earth. The availability of satellite imagery from the different remote sensing sensors (Table 1), at far lower costs per square kilometre than aerial photography and repeatable coverage now makes the use of remote sensing data not only technically advantageous but also economically preferable. The satellite remote sensing approach has already been used worldwide for oil exploration, and results published (V.T. Jones III, M.D. Matthews and D.M. Richers, 1999).

However, it is not yet well established in the world which benefit remote sensing may bring to oil exploration in general. Because of oil production and desertic environment, Libya is a good example for demonstrating the efficiency of satellite remote sensing approach for oil exploration.

The remote sensing analysis of Earth Observation (EO) data for the surface expression of subsurface structures is a very cost-effective method for a refinement of the interpretation of sub-surface data for the geometry, interaction, timing and distribution of structures, lithological and sedimentary features.

3.4.1 Mosaic Landsat TM5 Images

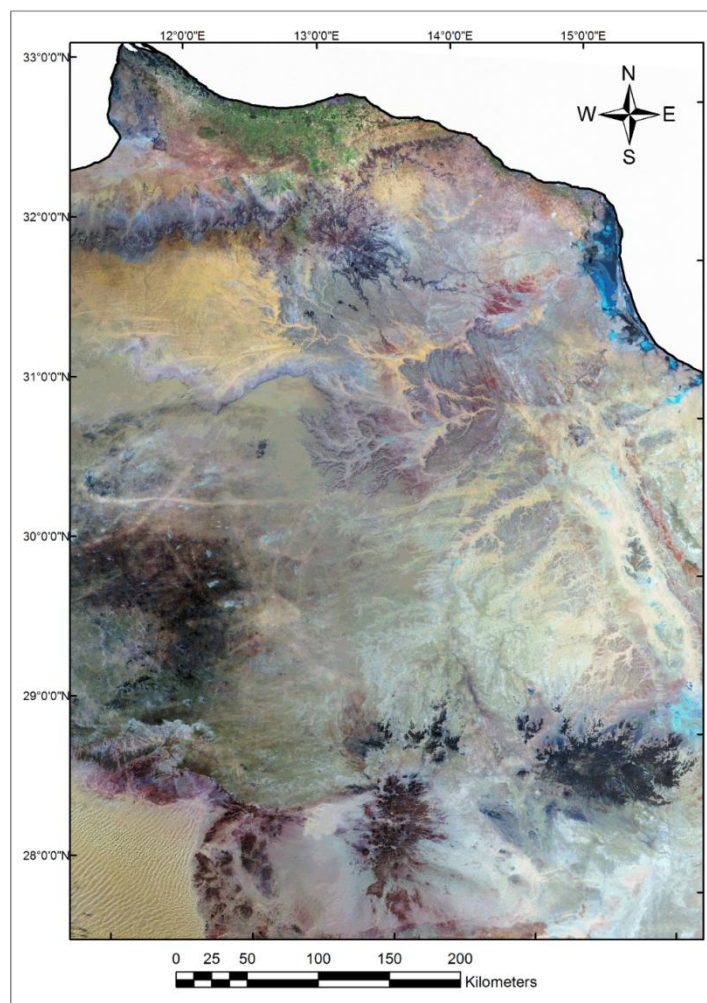


Figure 4: Mosaic Landsat TM 5 of the study area

Five Landsat have been launched since, the last unsuccessfully. The Thematic Mapper sensor, which was introduced on Landsat-4, sent up in 1982, produced images of considerable interest to the geologist. Landsat-5 was launched March 4, 1984, since Landsat-4 had been having problems; Landsat-6 was never heard from again after launch.

The MSS and TM sensors primarily detect reflected radiation from the Earth's surface in the visible and near-infrared (IR) wavelengths, but the TM sensor with its seven spectral bands provides more radiometric information than the MSS sensor. The wavelength range for the TM sensor is from the visible, through the mid-IR, into the thermal-IR portion of the electromagnetic spectrum. Sixteen detectors

for the visible and mid-IR wavelength bands in the TM sensor provide 16 scan lines on each active scan. Four detectors for the thermal-IR band provide four scan lines on each active scan.

The TM sensor has a spatial resolution of 30 meters for bands 1 through 5, and band 7, and a spatial resolution of 120 meters for band 6. All five of the Landsat have been in Sun-synchronous orbits with equatorial crossing times ranging from 8:30 a.m. A Landsat-4 or -5 TM scenes has an instantaneous field of view (IFOV) of 30 X 30 meters (900 square meters) in bands 1 through 5 and band 7, and an IFOV of 120 X 120 meters (14,400 square meters) on the ground in band 6.

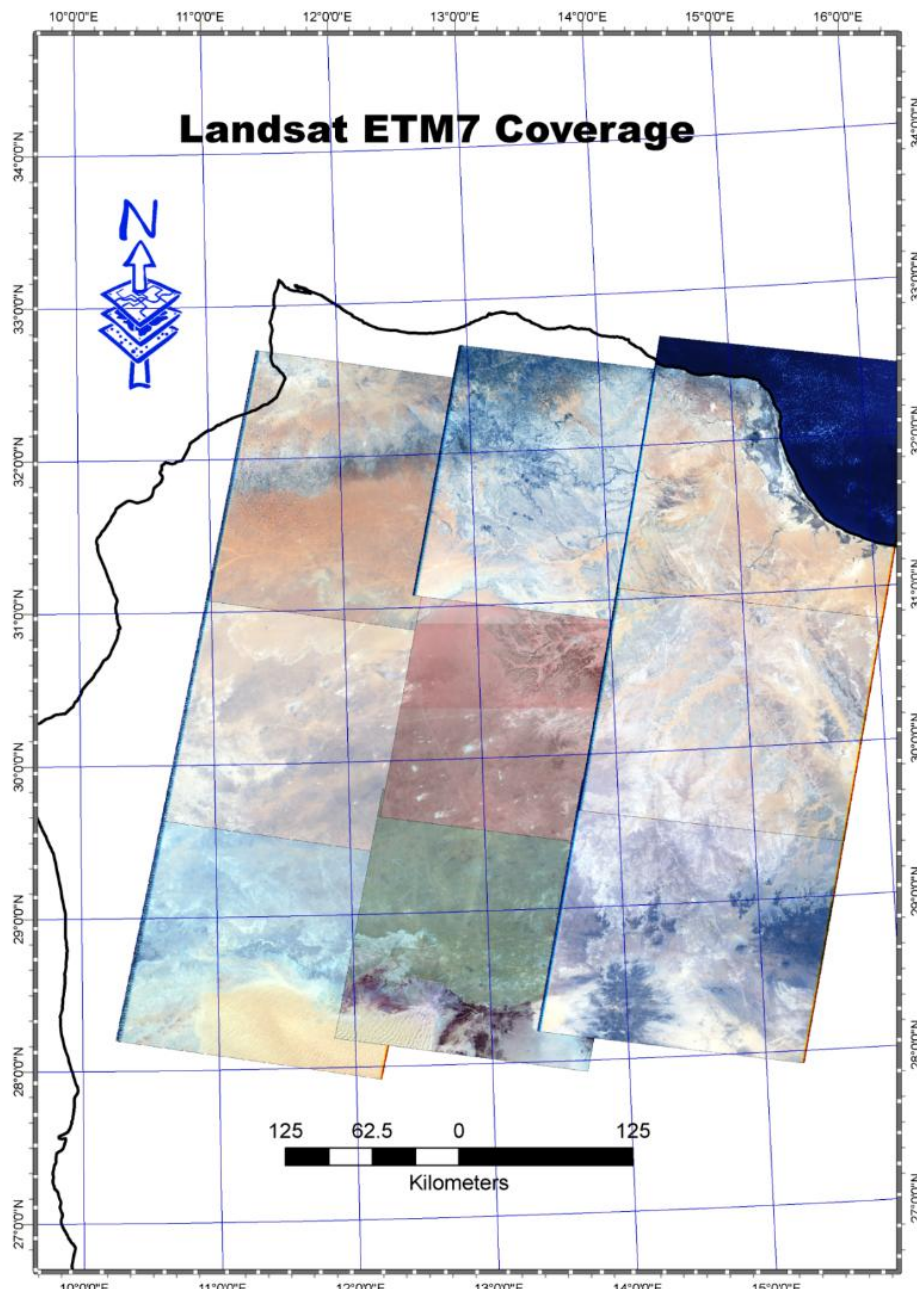


Figure 5: Landsat ETM 7 of the study area

The characteristics of the MSS and TM bands were selected to maximize detecting and monitoring different types of Earth resources. For example, band 1 of TM data penetrates water for bathymetric mapping along coastal areas and is

useful for soil-vegetation differentiation and for distinguishing forest types. TM band 2 detects green reflectance from healthy vegetation, and TM band 3 is designed for detecting chlorophyll absorption in vegetation.

TM Band 4 data is ideal for detecting near-IR reflectance peaks in healthy green vegetation and for detecting water-land interfaces. The two mid-IR red bands on TM (bands 5 and 7) are useful for vegetation and soil moisture studies and for discriminating between rock and mineral types. The thermal-IR band on TM (band 6) is designed to assist in thermal mapping, and is used for soil moisture and Vegetation studies.

Typically as used in this study, TM Bands 2, 4, 7 and 8, can be combined to make false-color composite images for geological mapping where band 7 represents the red, band 4 represents the green, and band 7 represents the red portions of the electromagnetic spectrum and band 8 (grey colour), represents as an Intensity layer to merge all the bands as 15 m. resolution.

The TM sensor is an advanced, multispectral scanning, Earth resources instrument designed to achieve higher image resolution, sharper spectral separation, improved geometric fidelity, and greater radiometric accuracy and resolution than the MSS sensor. The TM data are scanned simultaneously in seven spectral bands. Band 6 scans thermal (heat) infrared radiation. Spectral range of bands and spatial resolution for the TM sensor (Table 2) are:

Table 2: Spectral range of bands and spatial resolution for the TM sensor

Band	Wavelength (µm)	Spatial Resolution	Characteristics
1	0.45 - 0.52	30 metres	Blue-green: Maximum penetration of water, which is useful for bathymetric mapping in shallow water. Useful for distinguishing soil from vegetation and deciduous from coniferous plants. (blue)
2	0.52 - 0.60	30 metres	Green: Matches green reflectance peak of vegetation, which is useful for assessing plant vigour. (green)
3	0.63 - 0.69	30 metres	Red: Matches a chlorophyll absorption band that is important for discriminating vegetation types. (red)
4	0.76 - 0.90	30 metres	Reflected IR: Useful for determining biomass content and for mapping shorelines. (near infra-red)
5	1.55 - 1.75	30 metres	Reflected IR: Indicates moisture content of soil and Vegetation. Penetrates thin clouds. Good contrast. Between vegetation types. (infra-red)
6	10.40 - 12.50	120 metres	Thermal IR: Night-time images useful for thermal mapping and for estimating soil moisture. (thermal IR)
7	2.08 - 2.35	30 metres	Reflected IR: Coincides with an absorption band caused by hydroxyl ions in minerals. Ratios of bands 5 and 7 potentially useful for mapping hydrothermally altered rocks associated with mineral deposits. (near infra-red)

The Landsat TM data was digitally enhanced. Bands 7 (Mid Infrared), 4 (short wave infrared) and 2 (visible green) were selected and displayed as red, green and blue respectively to produce a false colour composite image. This band combination provides the best lithological discrimination. Band 2 was chosen in preference to band 1 to minimise the

effects of atmospheric haze particularly in coastal areas. A digital copy of the Landsat TM mosaic is supplied as part of this study.

3.4.2 SPOT XS (Satellite Pour l'Observation de la Terre)
 SPOT (Système Probatoire d'Observation de la Terre) was launched in 1986 (10m. resolution, as against MSS 80m and TM 30m resolution).

The SPOT satellites have identical orbits and sensor systems. The orbital altitude of SPOT is 832 km, and the sun-synchronous orbit is similar to that of Landsat. SPOT employs a high-resolution visible image system that can operate in high-resolution panchromatic or multispectral mode (Figure 6), these are:

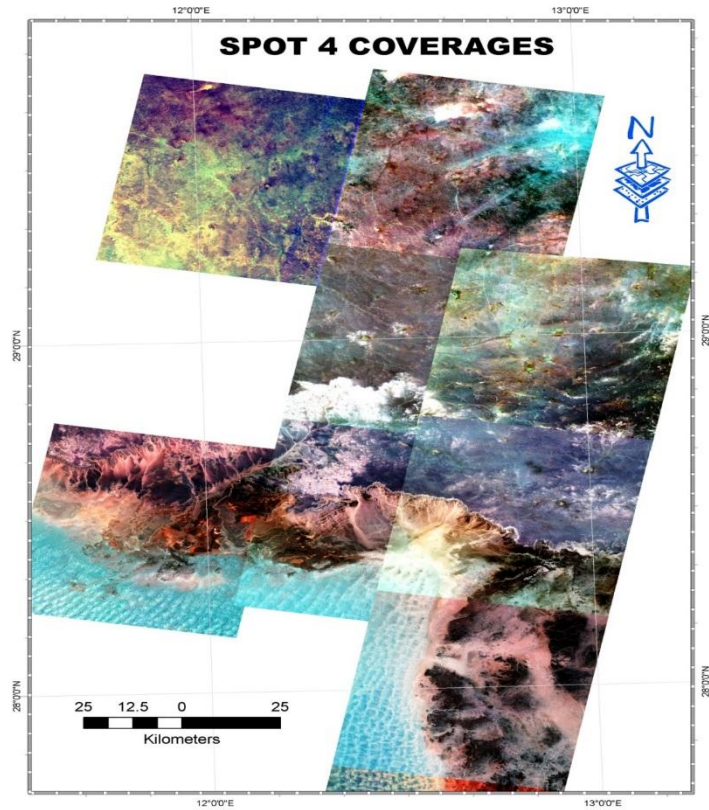


Figure 6: Coverage of SPOT 4.

- 1) Panchromatic mode with 10 meters of spatial resolution; the image is acquired in a single spectral band corresponding to the visible wavelength (0.51-0.73 microns). These images are used in applications where high geometrical resolution is needed.
- 2) Multispectral mode with 5 and 20 meters resolution (Figures 6 and 7). This mode contains 3 spectral bands: green (0.5-0.59 microns), red (0.61-0.68 microns) and near infrared (0.79-0.89 microns) whose selection has been optimised to allow maximal discrimination of various types of terrestrial targets.



Figure 7: Coverage of SPOT 5.

The SPOT instrument package has the provision for off-nadir viewing which should be particularly useful for monitoring localized phenomena evolving on a relatively short timescale. SPOT, also, provides the capability for recording stereoscopic pairs of images of a given area during successive satellite passes. The main applications for the images returned by the first SPOT mission are land-use studies, agriculture and forestry resources, mineral and hydrocarbon exploration, and cartography.

3.4.3 Radar Imagines

Radar is an active sensor, using the emission and analysis of returned waves; these pulses are from a millimetre to a meter in wavelength and in the case of radar carried by airplanes are emitted from a sensor in the side of the craft. The radar pulses outward in a fanlike beam beneath the aircraft, with the plane of the fan perpendicular to the flight direction of the aircraft. Rough surfaces look bright and smooth surfaces look dark in a radar image; high mountains or tall buildings block the signal and thus cast "shadows" on an image. Dense vegetation can also produce some shadowing effect. SLAR

(Side-Looking Airborne Radar) is a valuable tool for geologic analysis (for structure and tectonic interpretation), especially for petroleum and mineral exploration; it shows topography well because of the angle of incidence of the radar beam.

- Its cloud-penetration capability makes it especially valuable for areas where conventional aerial photographs are difficult to acquire SLAR, 1985.
- Images are in long, broad strips, giving unbroken coverage, unlike working with aerial photographs
- SLAR accentuates linear features and defines faulting patterns
- Subtle lithological changes may sometimes be depicted very clearly
- Radar signals penetrate a short distance into dry soils; for X and K band (normally used for SLAR), this really is a short distance, a millimetre or a fraction of a millimetre (Barringer, 1970)

The ERS (European Remote Sensing Satellite) is an active sensor which allowing data to be collected both day and night. The sensor then processes the backscatter signal that it receives back from the earth's surface. Areas of low backscatter appear relatively dark whereas areas of high backscatter appear relatively bright (Figure8).

ERS data has the advantage of enhancing topography and textural variations which helps to highlight subtle geological structures such as faults, low amplitude folds and changes in the dip of bedding, which are not always visible on the Landsat TM imagery. In ideal cases, ERS data also provides a limited amount of penetration (less than 100cm.) through dry granular overburden.

Radar provides its own source of illumination and unlike optical remote sensing is not constrained by poor weather (e.g., clouds and dust storms) or sunlight conditions. Thus, SAR can collect data over virtually any region at any time. Radar remote sensing uses the microwave portion of the electromagnetic spectrum from a frequency of 0.3 to 300 GHz, corresponding to wavelengths of 1m. - 1mm. Four main frequencies are currently used for satellite remote sensing:

- 1) X-band uses a wavelength range of 2.4 to 3.8 cm (12.5 to 8 GHz).
- 2) C-band uses a wavelength range of 3.8 to 7.5 cm. (8 to 4 GHz).
- 3) S-band uses a wavelength range of 7.5 to 15 cm (4 to 2 GHz).
- 4) L-band uses a wavelength range of 15 to 30 cm (2 to 1 GHz).

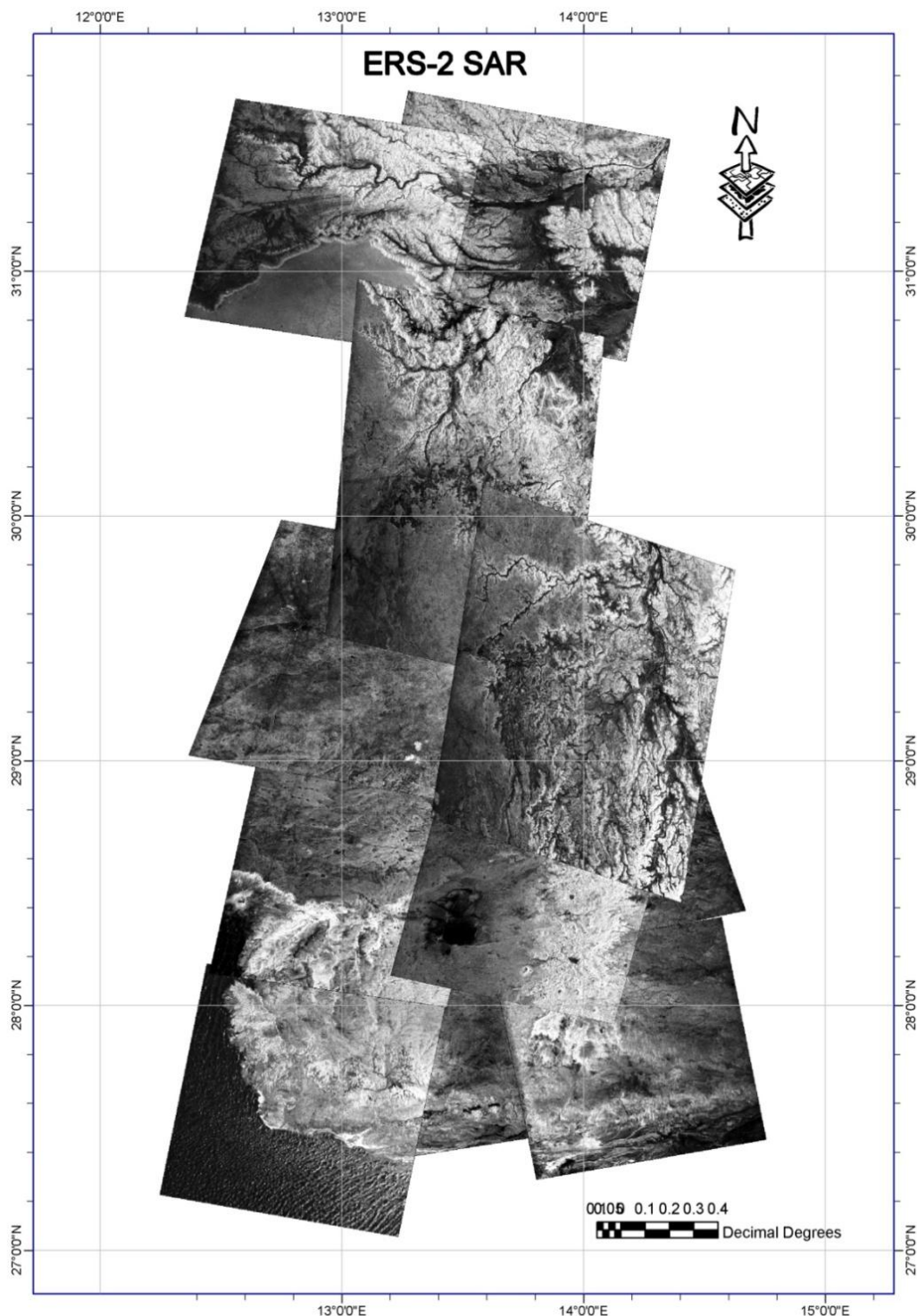


Figure 8: Coverage of ERS-2 SAR

Radar introduces a whole new dimension to satellite remote sensing that is not possible with optical imagery. Radar can provide information about the earth's surface that is related to topography, surface roughness, and moisture conditions. In addition, the long wavelengths used by radar permit limited penetration beneath dry surface materials, such as sand, to sense the underlying conditions.

The application of SAR to surface or geological mapping depends upon the frequency, polarization, spatial resolution, look-direction, incidence angle, swath width and image processing depth. The information available from microwave remote sensing is different from but

complimentary to that available from the visible and IR wavelengths. In arid desert environments, a major advantage of using SAR in desert environments is its ability to penetrate sand dunes and expose hidden structures.

SAR's ability to differentiate between land-use and land cover types due to different surface roughness, volumetric backscattering and moisture regimes. ERS-2 is a remote sensing satellite launched by the European Space Agency carrying Synthetic Aperture Radar instrument, which is used to image the Earth's surface. The ERS-2 SAR is a C-band (6 cm wavelength) instrument, operating with VV Polarisation. Its orbit height is about 800 km and range of incident angles

within a typical image is fixed at between 20° for near range and 26° for range. A typical image area is 80X80 km. The ERS SAR imagery was enhanced for maximum interpretability and mosaic.

A filter-sar\std-dev-1.6 ker was applied to the imagery to decrease the amount of speckle inherent in the data. The ERS data helps to identify structures not visible on the optical Landsat TM imagery by emphasising subtle variations in topography and texture of the surface materials. The C-band of ERS satellite imagery also provides a limited amount of penetration through dry granular surface materials down to 100cm. (dependent on grain size, mineralogy, amount of compaction). This also helps to identify geological structures obscured by thin dry sand overburden (Figure 8).

3.4.4 Google Earth

Google Earth is available on the web for free, the free version offers numerous features that are useful in educational settings, the Pro-version offers additional capabilities such as higher resolution printing and saving of images and the ability to open ESRI shape-files. Google Earth is a geo-browser that accesses satellite and aerial imagery, geographic data over the internet to represent the Earth as a three-dimensional globe (Figure 9).

Google Earth is an interactive mapping application that allows users to navigate (or "fly") the entire globe, viewing satellite imagery with overlays of roads, buildings, geographic features. Google Earth now hosts high-resolution imagery that spans 20% of the Earth's landmass and more than a third of the human population. This contemporary high resolution archive represents a significant, rapidly

expanding, cost-free and largely unexploited resource for scientific inquiry.

Landsat Geo-Cover is an ortho-rectified product with known absolute positional accuracy of less than 50 meters root-mean-squared error (RMSE). Relative to Landsat Geo-Cover, the 436 Google Earth control points have a positional accuracy of 39.7 meters RMSE (error magnitudes range from 0.4 to 171.6 meters). The control points derived from satellite imagery have an accuracy of 22.8 meters RMSE, which is significantly more accurate than the 48 control-points based on aerial photography (41.3 meters RMSE; t-test p-value < 0.01).

The accuracy of control points in more-developed countries is 24.1 meters RMSE, which is significantly more accurate than the control points in developing countries (44.4 meters RMSE; t-test p-value < 0.01). These findings indicate that Google Earth high resolution imagery has a horizontal positional accuracy that is sufficient for assessing moderate-resolution remote sensing products.

The goals of using the Google Earth in our case of study:

- 1) We used the Google Earth high resolution imagery for interpretation of geometry of planar dipping layers from the outcrop pattern (Folded areas).
- 2) We used the Google Earth to recognize different rock units based on their characteristics as seen on satellite images.
- 3) We used the Google Earth to draw geological maps and interpret structure based on the map pattern of different units (Figure 9).



Figure 9: close-view of Google Earth, the border of Sirt Basin and Ghadamis Basin, extension fault, parallel to Hun Graben NW-SE direction, the dipping to the East (Ghadamis Basin). Vertical Exaggeration 3x.

The approach that we used:

- We started with the planar contacts in areas which having not good topography.
- We defined some of strike and dip and the various types of the Formations contacts.
- We using 3D topographic relief, to define the outcrop pattern of horizontal contacts, moving-on to vertical contacts, and then address inclined contacts and derive the rule of V-shape, (Anticline and/or Syncline).
- We used the Google earth by moving-on to maps with folded contacts.
- We using the Google Earth 3D view to develop an understanding of dip and use Google Earth 3D view to help us for visualize the relationships and, finally, for **folded and faulted contacts**.

Google Earth provides search capabilities and the ability to pan, zoom, rotate, and tilt the view of the Earth. It also offers tools for creating new data and a growing set of layers of data, such as volcanoes and terrain that reside on Google's servers, and can be displayed in the view.

It also uses elevation data primarily from NASA's 'Shuttle Radar Topography Mission' (SRTM) to offer a terrain layer, which can visualize the landscape in 3D. For some locations, the terrain data is provided at significantly higher resolutions (Figure 10).

Google Earth is not a Geographic Information System (GIS) with the extensive analytical capabilities of ArcGIS or MapInfo, but is much easier to use than these software packages.

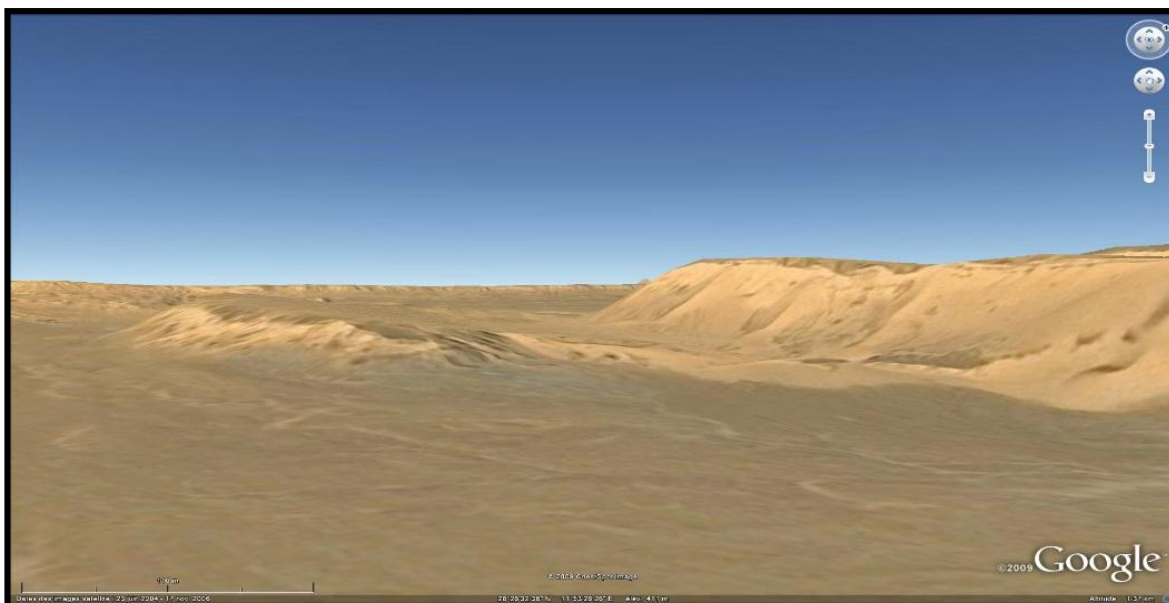


Figure 10: 3D Google Earth, NE border of Ghadamis Basin, NNW extension Fault, parallel to Hun Graben

3.4.5 ENVI-SAT

The objective of the Envisat programme is to enhance capability for remote sensing observation of Earth from space, with the aim of further increasing the studying and monitoring of the Earth and its environment. Its primary objectives are:

- To provide for continuity of the observations started with the ERS satellites, including those obtained from radar-based observations;
- To enhance the ERS mission.
- To extend the range of parameters observed to meet the need of increasing knowledge of the factors determining the environment;
- To make a significant contribution to environmental studies. These are coupled with two linked secondary objectives:
 - To allow more effective monitoring and management of the Earth's resources;
 - To better understand solid Earth processes.

The mission intends to continue and improve upon measurements initiated by ERS-1 and ERS-2, and to take into account the requirements related to the global study and monitoring of the environment.

Envi-sat, as an undertaking of ESA member states plus Canada, constitutes a major contribution to the international effort of space agencies worldwide to provide the data and information required to further the understanding, modeling, and prediction of environmental and climatic changes.

This mission includes both global and regional mission objectives, with the corresponding need to provide data to scientific and applications users on various time scales.

4. Satellite Data and Image processing methods

4.1 Digital Image Analysis

Spectral and textural information provide excellent interpretative assistance through the use of remote sensing images. When viewing various images the interpreters can readily see difference rocks, etc. Digital image processing permits the interpreter to go beyond the intuitive classification of such features and quantify specific target features using appropriate image processing software.

The digital image analysis of Landsat TM, Spot XS and ERS-2 data was performed using ER-Mapper Image processing. The Various digital techniques employed for

processing the images includes band combination (7,4 and 2 plus 8 as Red, Green, Blue and Intensity layer) for Landsat ETM7 images, and (3, 2 and 1 as Red, Green and Blue) for Spot XS images. ERS-2 images were processed using Erdas image processing to enhance the textural information in the area such as faults, Joints, Folds and silicified zones (Sedimentary Dikes). This digital mosaic allows also digital enhancements (e.g., sharpening lineaments and edges of features, increasing contrast and range of tone or hue, etc.); and compatible with multi-scale analysis and choice of optimal scale for study identification with the zoom facilities of the software.

4.2 Georeferencing

The Landsat TM data was georeferenced to geographical (lat.& long.). The georeferencing accuracy in the x and y directions is +/- 500 meters. As a first step of the digital integration of spatial data, geometric correction and co-registration of all data types on a common cartographic projection has been applied. The Geo-coding source: 1:500 000 TPC's, the Projection information as follows: Grid: UTM zone 32 north, Geodetic Datum: WGS 84, Central meridian: 9° East, Latitude of origin: equator, False Eastings: 500 000 meters, False Northings: 0 meters and Scale factor: 0.9996 was used. The Landsat TM5&7, Spot4 XS and ERS-2 images were geometrically corrected by an image to map registration procedure (Table 1). The individual Landsat TM scenes were edge-matched to form a single image mosaic. The ERS SAR data was georeferenced to the warped Landsat TM imagery.

5. Geographic Information System (GIS) Data

5.1 Database

Geographic Information Systems (GIS) are becoming a widely accepted tool in exploration. Because GIS is spatially based, it is a natural working environment for the exploration. It gives the user the opportunity to integrate a wide variety of different data and, importantly, allows non-specialists to perform sophisticated queries from associated databases. Also, that all of the thematic data and data tables can be edited and new data can easily be integrated. The variety of different data themes including:

Point Data - Typically these will contain e.g. Well Locations which will be linked to other tables.

Line Data - Usually contours for structure, Isopach, Gravity, Magnetics etc.

Polygon Data - This data type can include concession areas, geological maps and distribution. Polygon themes are also used for cross-sections and stratigraphic correlation diagrams.

Other data types used are grids and raster images. An important new development is the use of geo-rectified raster data in this study. These geo-rectified images can be satellite imagery or scanned maps. The importance of geo-rectification is that data are converted to real world co-ordinates and can therefore be displayed as a backdrop with other themes, i.e. satellite imagery can be overlain with surface geology, fields and wells, or published geological

map image could be displayed against vectorised gravity data.

The amount of data already acquired by all means is so considerable that it is now necessary to store information in the frame of geographic information system (GIS), in order to make them easily available to all types of researchers. GISs are already in use e.g., report of Consultant Australian company (SRK), but progress is needed to render them more completed, efficient, and to complete the information by introduction of remote sensing data and their specific interpretation and to conducting an up-to-date assessment of the Ghadamis Basin. I have got authorization to get a copy of the necessary data and reports for the duration of this study.

The main job in this part more specifically, to carry out a fully integration study of the existing and available geological and geophysical information accessed at the National Oil Corporation of Libya, also to settle a permanent Database. All technical work was performed by different licenses software, insuring a good coherence and conformity in the interpreted data. The fulfillment of these objectives has been facilitated by experienced professional of Prof. Jean CHOROWICZ and access to sophisticated software. Integrate the result of such study with other geologic and thematic data by applying geographic information systems (GIS). Integration of remote sensing data of different spatial and/or spectral characteristics and digital elevation models (DEM) can extremely effective in mapping morphologically-defined structures.

5.2 GIS and remote sensing activity involved:

- Acquisition and processing of 15 scenes of Landsat ETM7 satellite imagery and production of a georeferenced digital mosaic (Figure 5).
- Acquisition and processing of 12 scenes of ERS-2 SAR (synthetic aperture radar) and production of a georeferenced digital mosaic (Figure 8).
- Generation of a merged Landsat ETM7\ SAR satellite image mosaic (Figure 11).
- Generation of a merged Landsat TM 5\Geological Map (Figure 12).
- Generation of a merged ERS SAR / DEM satellite image mosaic (Figure 13).
- Generation of a merged DEM / Magnetic map satellite image mosaic (Figure 14).
- Generation of a merged ERS SAR / SPOT4 satellite image mosaic (Figure 15).
- Generation of a merged SPOT4/Landsat ETM7 satellite image mosaic (Figure 16).
- Generation of a merged ERS /Magnetic map satellite image mosaic (Figure 17).
- Structural geological interpretation of Landsat TM and ERS SAR satellite imagery.
- Integration of subsurface structure derived from interpreted seismic profiles and aeromagnetic image.

5.3 Merging different Remote Sensing Images and Ancillary data

a) Merged Landsat ETM7 and Radar (ERS-2)

The merged Landsat TM/ERS SAR image (Figure 11) was produced by displaying the enhanced ERS SAR data as an intensity layer and then merging it with the band 7,4,2 false

colour Landsat TM composite and 8 (Intensity layer). The merged imagery was plotted as a set of 12 encapsulated 1:250,000 scale image map sheets. The Spot and Landsat TM provide the spectral information while the Synthetic aperture radar ERS-2 data provides the textural information.

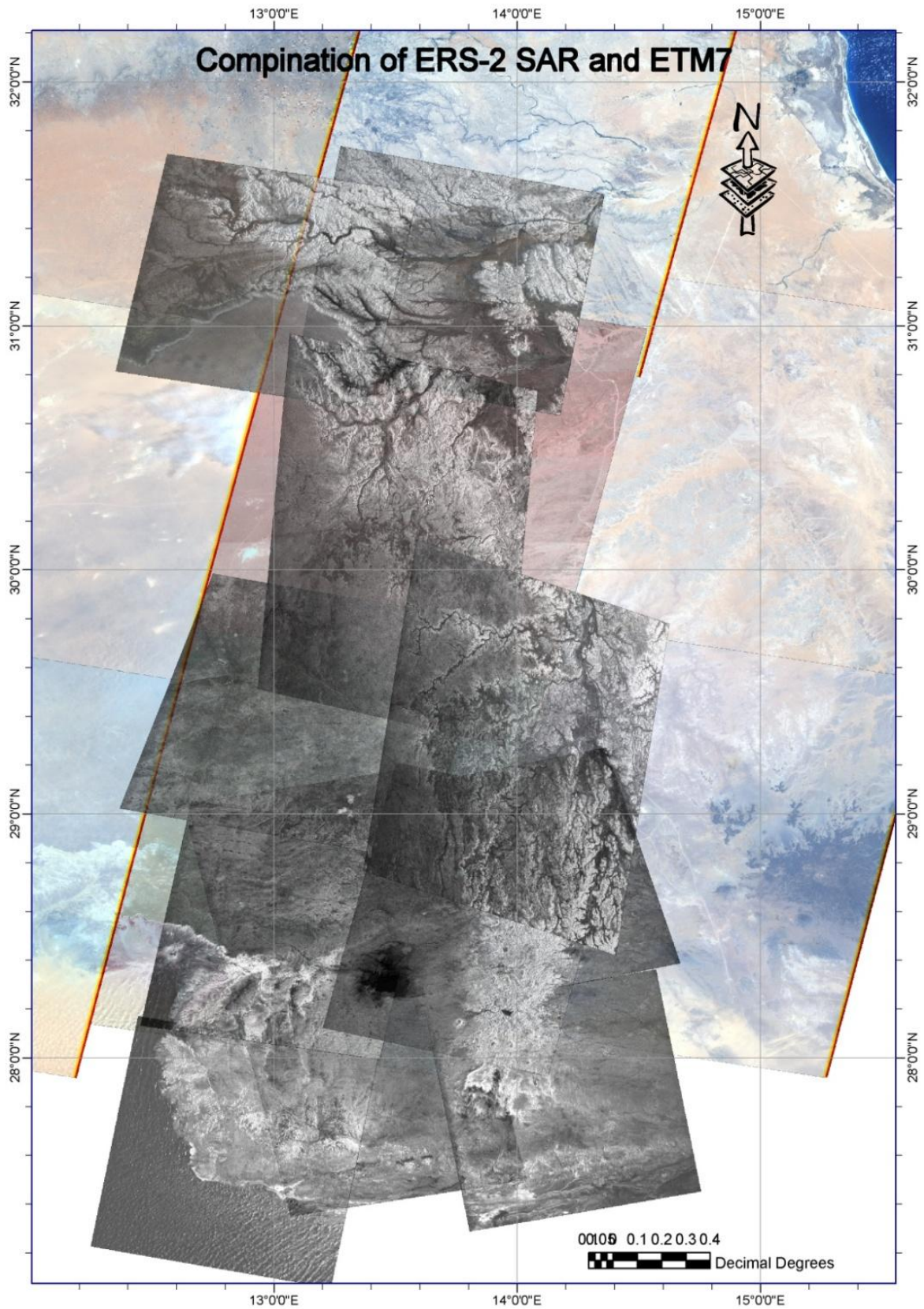


Figure 11: Combination of ERS-2 SAR and Landsat ETM 7.

The characterization of the terrain analysis, of rock units for the most cover area in Ghadamis Basin (Quaternary to Cambro-Ordovician), the comparison and merging of ERS and Landsat TM is described in the (Table 3).

The merged Landsat ETM7 and Radar (ERS-2) imagery covering the study area has been used to map surface geology and structures. Visual and digital satellite image analyses have enabled the rapid mapping of the regional tectonic structures and features while when merged with radar revealed additional and more detailed information.

It allowed precise delineation of the structural and topographical expressions of the fault block styles and the structural provinces boundaries. Folds are very rare with exception of very low amplitude anticlines and synclines (i.e. Geziel oil field).

Table 3: Description of the rock units of Ghadamis Basin by ERS and Landsat TM imageries

AGE	Colour on Merged 742 R,G,B Landsat TM/ERS SAR	Textural Characteristics (ERS-2 SAR)
Quaternary	Pale yellow, brown and grey	Smooth, low back scatter, medium – dark grey tone
Igneous Tertiary	Basaltic flows – dark brown	Smooth, low back scatter, medium-dark grey tone
Tertiary	Dark brown	Smooth to moderate, moderate back scatter, medium grey tone
Cretaceous	Greenish blue	Medium grey tone
Permian	Pale brown to reddish brown	Moderate rough, high back scatter light-medium grey tone
Carboniferous	Red to reddish brown	Smooth, low back scatter light -dark grey tone
Middle & Upper Devonian	Red to brown	Smooth, low back scatter medium-dark grey tone
lower Devonian	Dark green to brown	Rough, high back scatter light-medium grey tone
Silurian	Reddish brown	Rough, high back scatter light-medium grey tone

Ordovician	Pale dark brown and light brown	Moderate-rough, moderate back scatter light-medium grey tone
Cambrian - Ordovician	Very light blue	Highly – Moderate rough, moderate back scatter light-medium grey tone

b) Merge Landsat TM 5 \ Old Geological Map

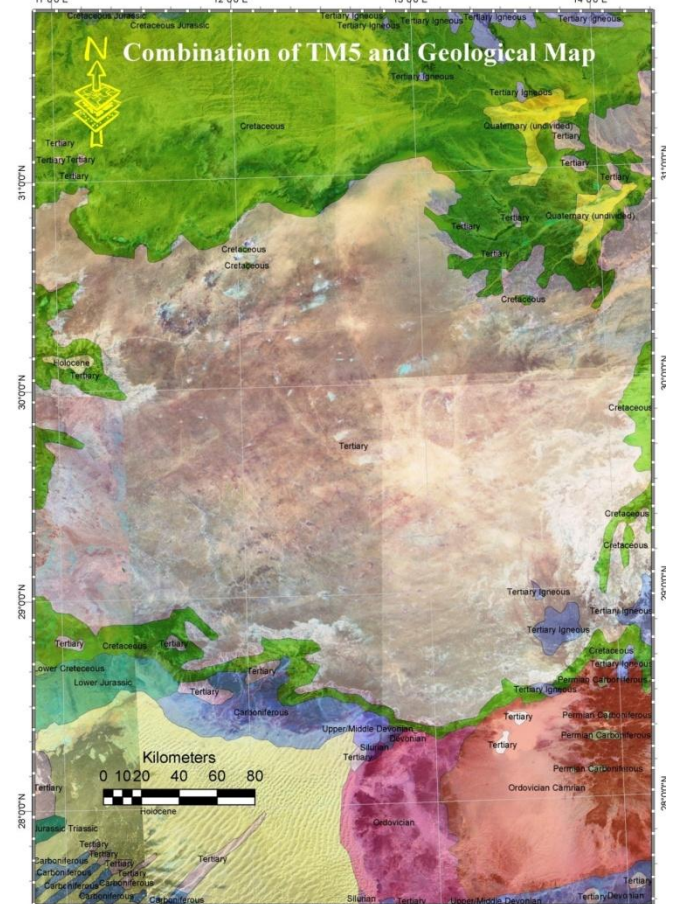


Figure 12: Combination of Geological map and Landsat TM 5.

c) Merge ERS-2SAR / DEM

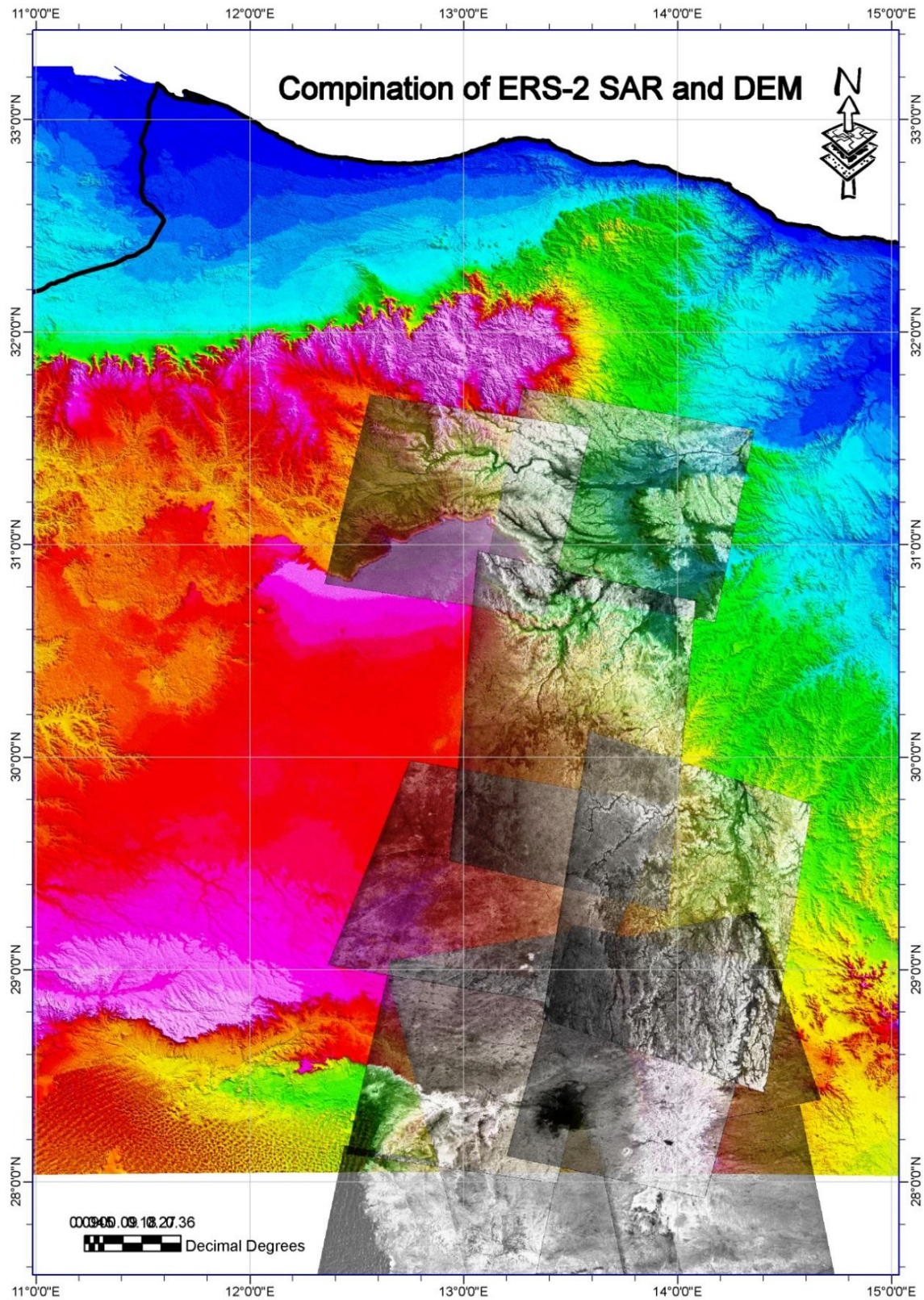


Figure 13: Combination of ERS-2 SAR and DEM

d) Merge DEM / Magnetic map

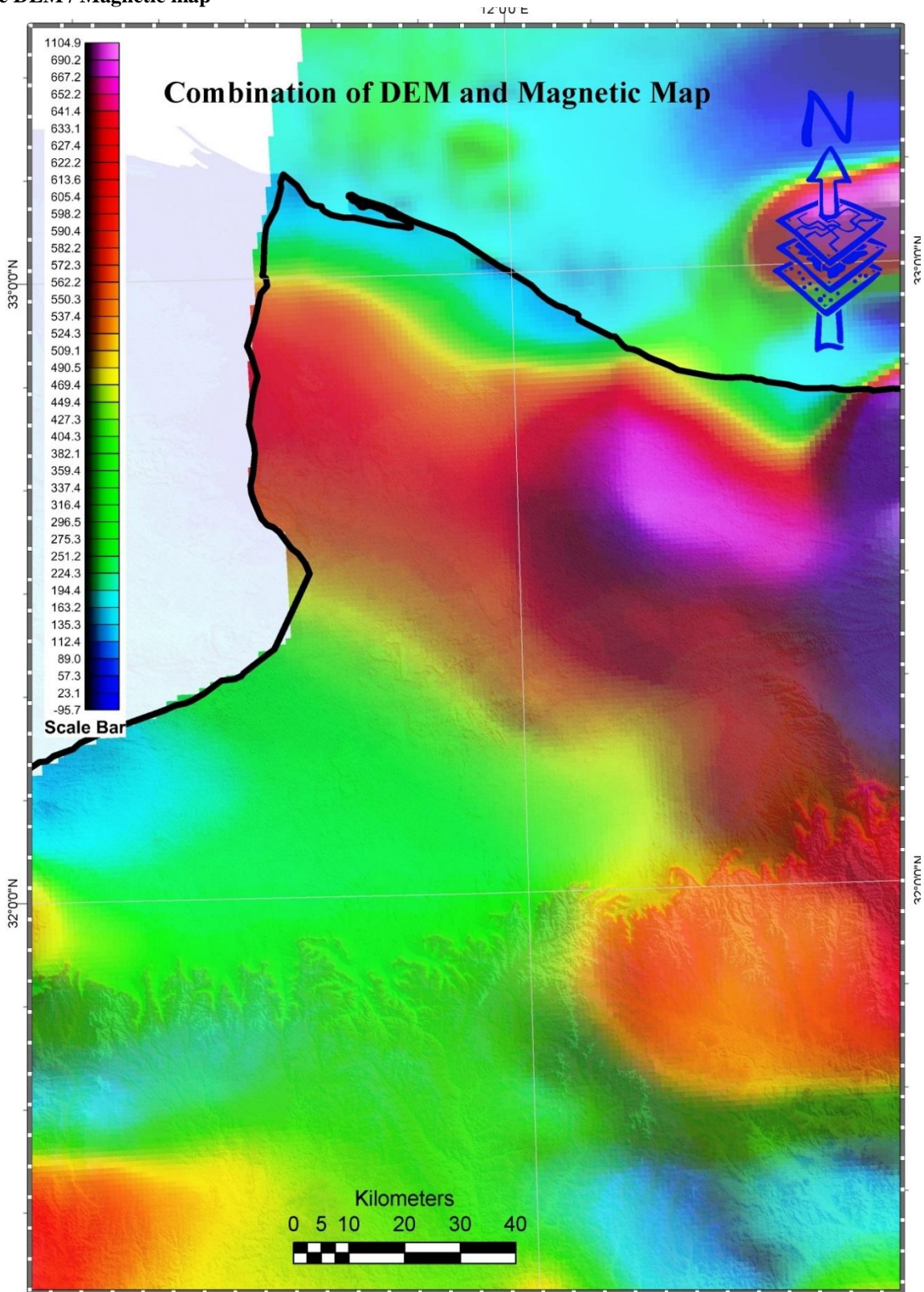


Figure 14: Combination of DEM / Magnetic map.

e) Merged ERS-2 SAR / SPOT 4

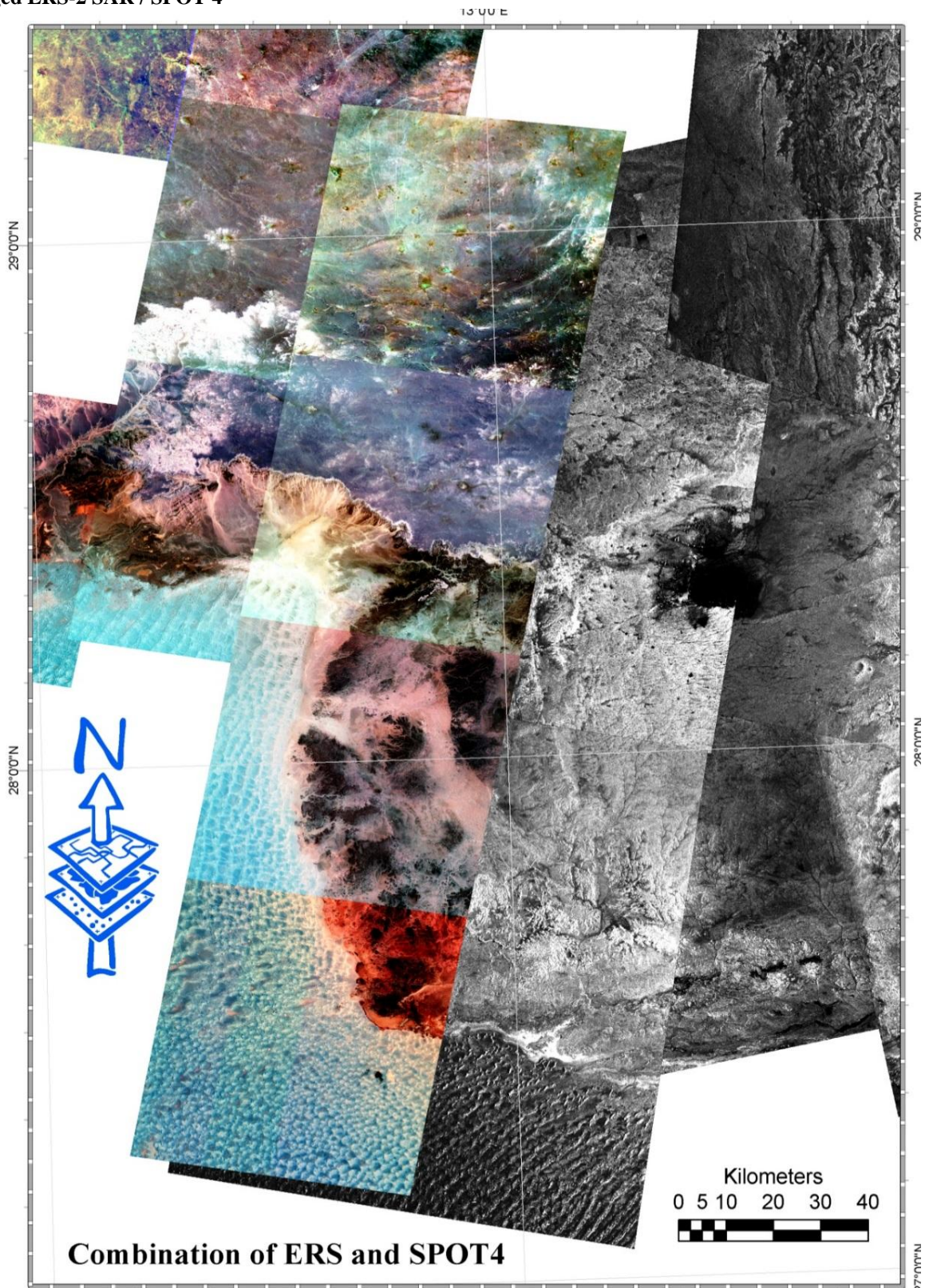


Figure 15: Combination of ERS-2 SAR / SPOT 4.

f) Merged SPOT 4 / Landsat ETM 7

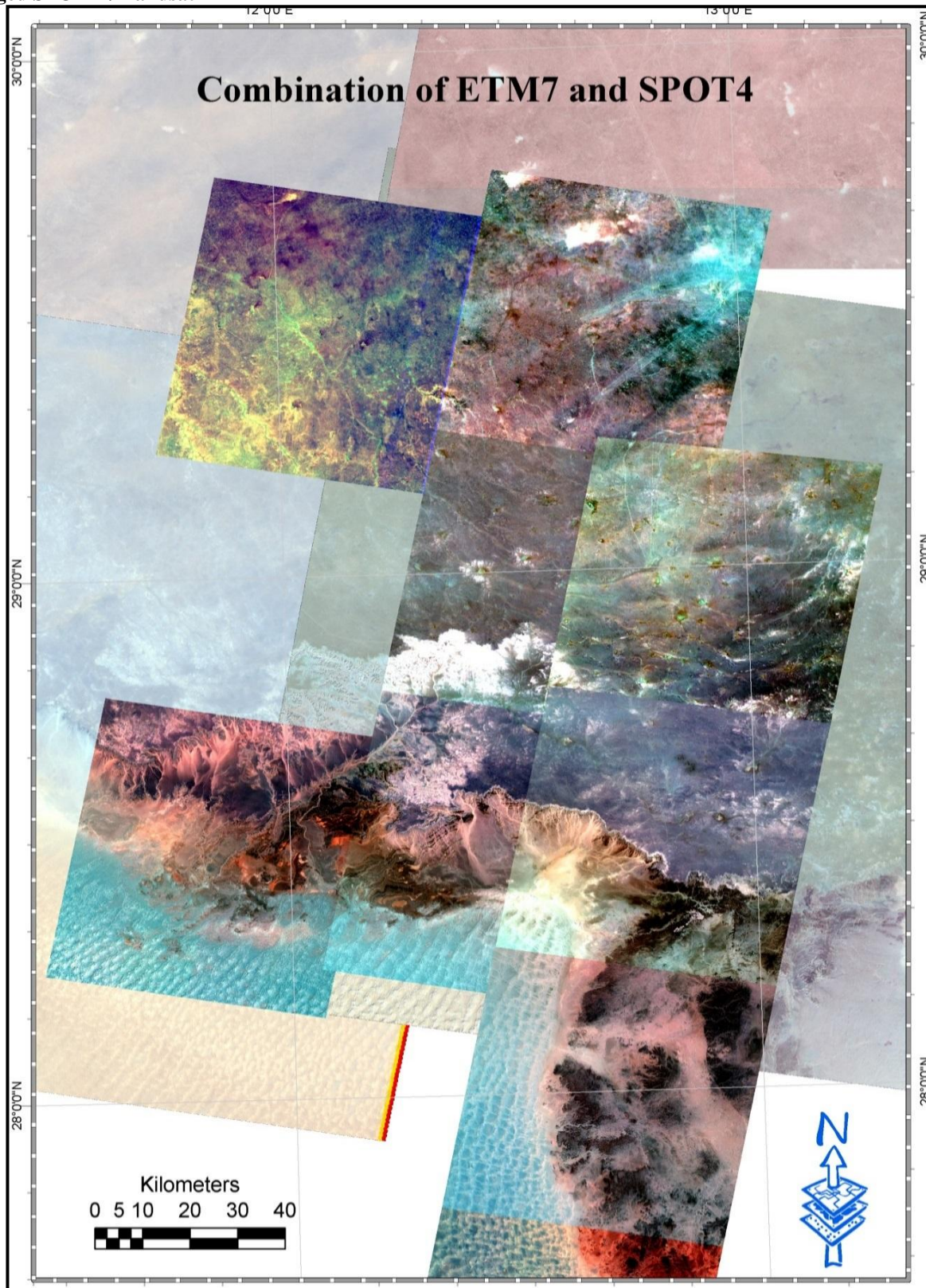


Figure 16: Combination of SPOT 4 / Landsat ETM 7.

g) Merged ERS-2 SAR / Magnetic map

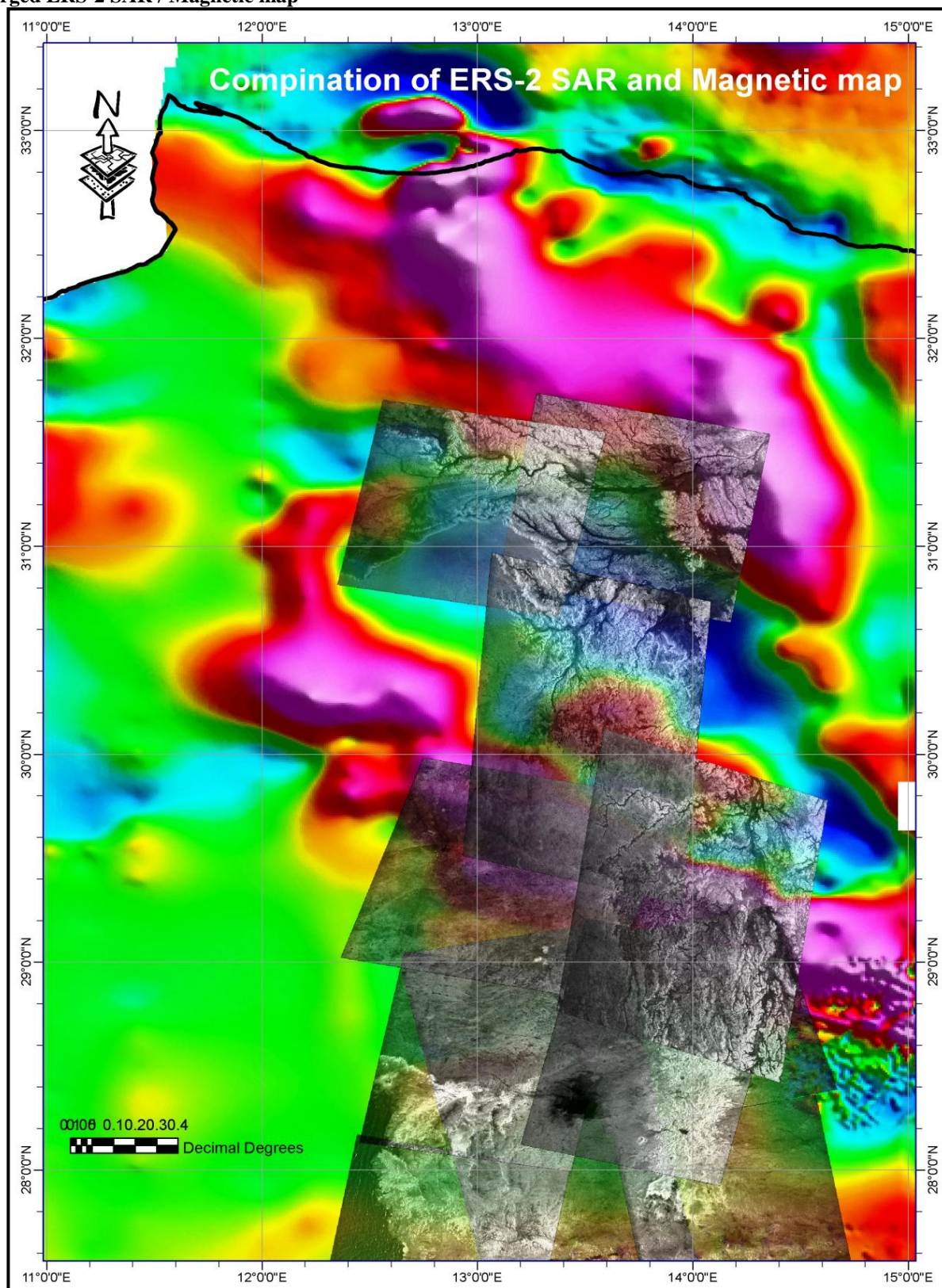


Figure 17: Combination of ERS-2 SAR / Magnetic map

6. Innovation: How to use the GIS database?

6.1 Application of sorting the data

a) Representation of the layers

Instead of representing polygons of outcrops, as is the case in conventional geological maps printed on paper (Ghanmi

et al., 1987), our GIS litho-stratigraphic map (Figure 18) is made on the basis of a new concept in which we represent each unit by the polygons of its base, projected on to the map (Figure 18). The polygons of the base of each unit are recorded in a given shape-file in (Figure 18).

The advantage of this method is the possibility to scorch off the map, unit after unit, showing that the information concerning the distribution of each unit is explicitly known not only on the surface but also in depth (Figure 18). When a unit is cut by a fault, the boundaries of the base of this unit express the cutting, implying a displacement, even when the unit is hidden in depth (Figure19).

In our case of study, estimate of the plunge of the layers, from strike-ridge morphology and topographic data using Google Earth 3D is to N210° azimuth, ~10°.

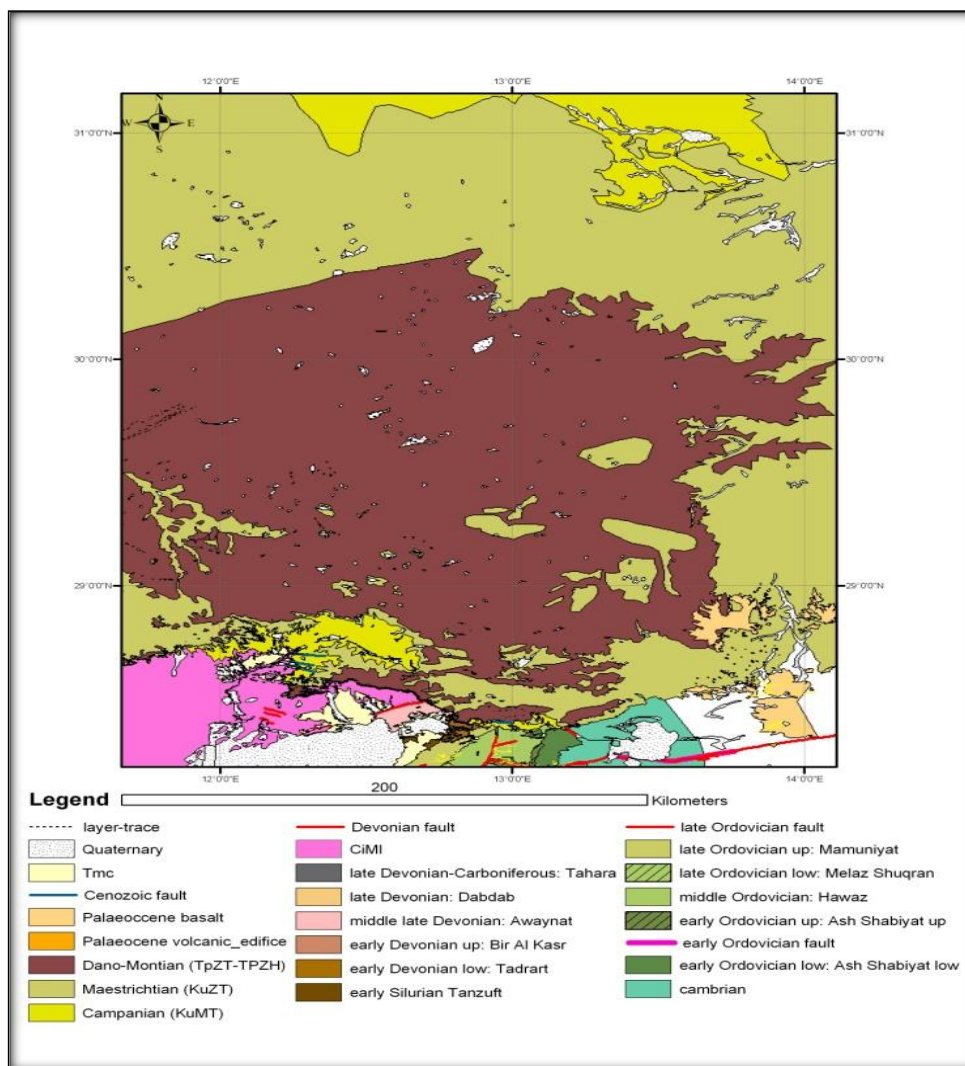


Figure 18: GIS litho-stratigraphic map.

The layers traces can be followed one by one using their observable line continuity and, when there is a doubt because of interruption of lines, they can be identified from

their morphologic context; we have restricted our layer traces analysis to that of this unit.

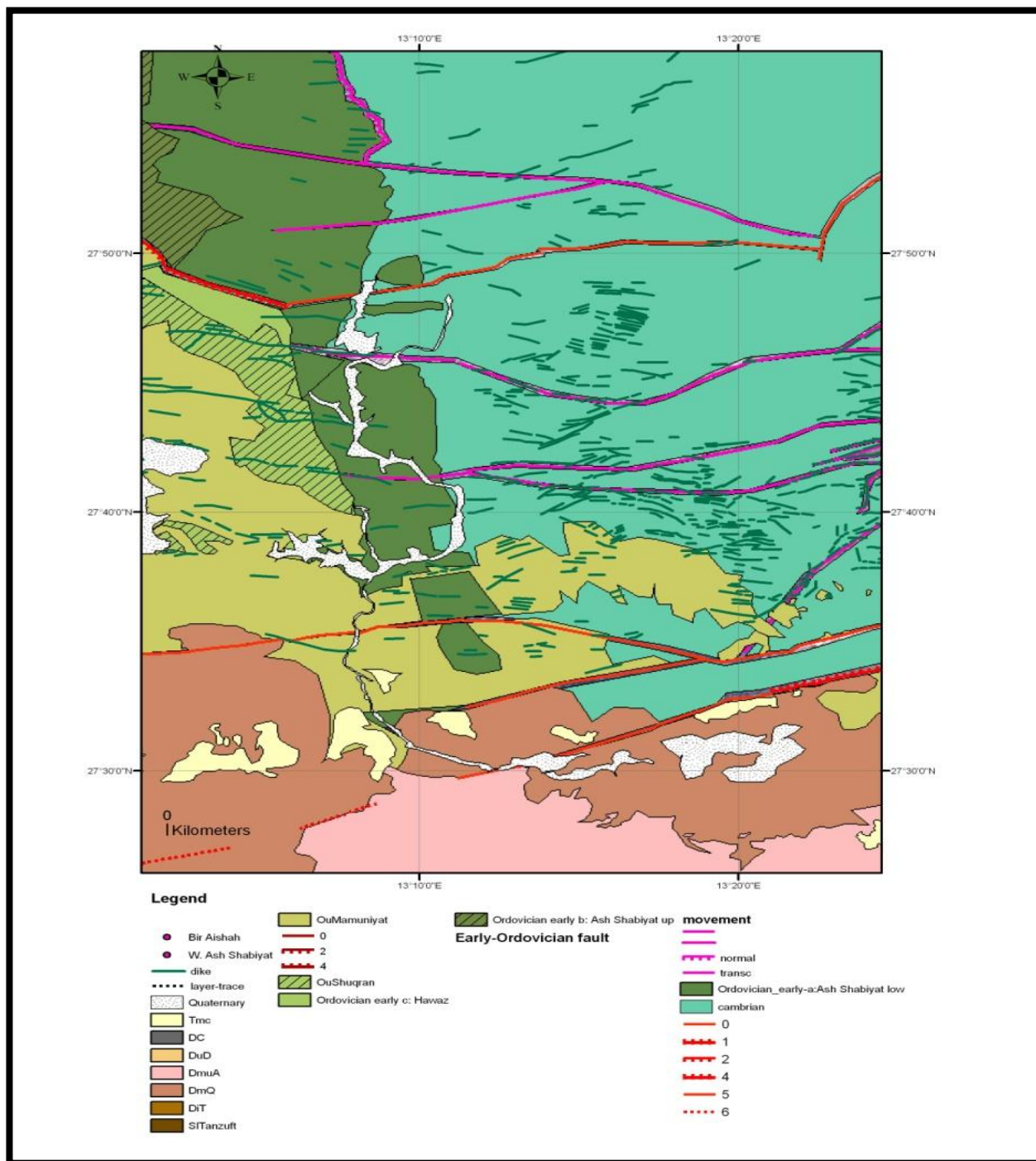


Figure19: Map showing layer traces analysis. The units are cut by the faults; the boundaries of the base of this unit express the cutting, implying a displacement, even when the unit is hidden in depth.

In order to make the maps readable, we have also restricted the number of layer traces to draw. The traces that can be followed easily are the bases of limestone units, because they correspond to the topographic expression of a break in slope at foot of a scarp.

It is generally more difficult to identify the boundaries between a limestone unit and the clay unit over it, the morphology being a progressive change in slope. Finally, we have preferably divided the Palaeozoic rocks into successions of units which comprise each a limestone group and the clay group over it. The boundaries between these units are considered as the layer traces to draw.

The geological maps obtained with the method used represent the units one by one with a shape-file each, showing the geology in depth by scorching off the map. The final outcrop map is the result of the superimposed GIS layers (Figures 18 and 19).

6.2 Updating of old maps and structural geology of area

Remote sensing analysis is an efficient tool for updating geological maps (Benissa, M. A. and J. Chorowicz, 2016). The regional scale map obtained in this study from compilation of the pre-existing maps and of a number of space images is somewhat more complete. It takes into

account the usual field and laboratory parameters of the rock units, through the previous geologic maps, together with remote sensing parameters such as spectral signatures, textures, roughness, morphology that are observed from

optical, microwave and DEM imagery. With more rock characteristics, the old maps are obligatory improved (Figures 20-24).

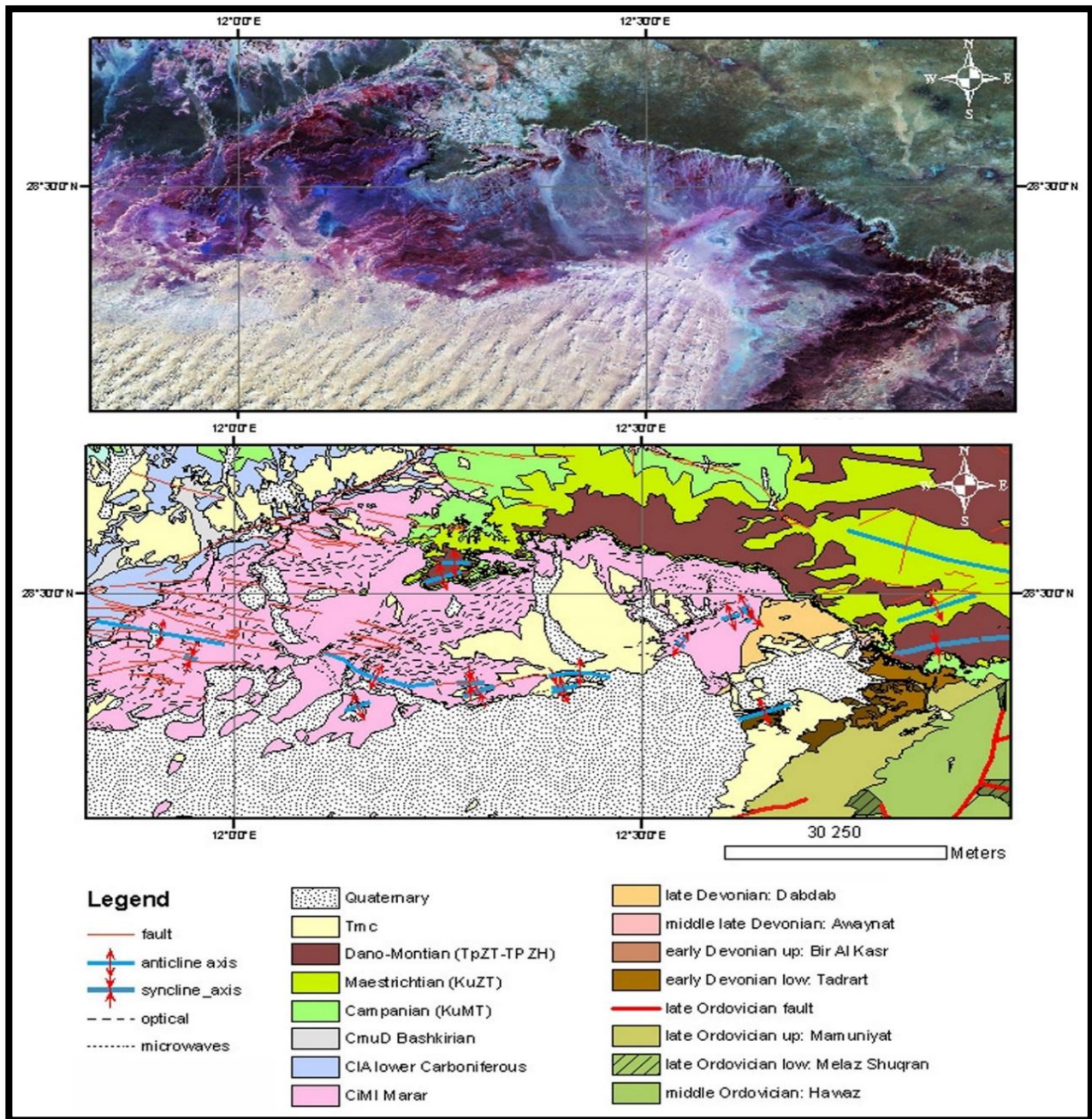


Figure 20: Updated geological map of Carboniferous outcrops, NW of Al Qarqaf arch.

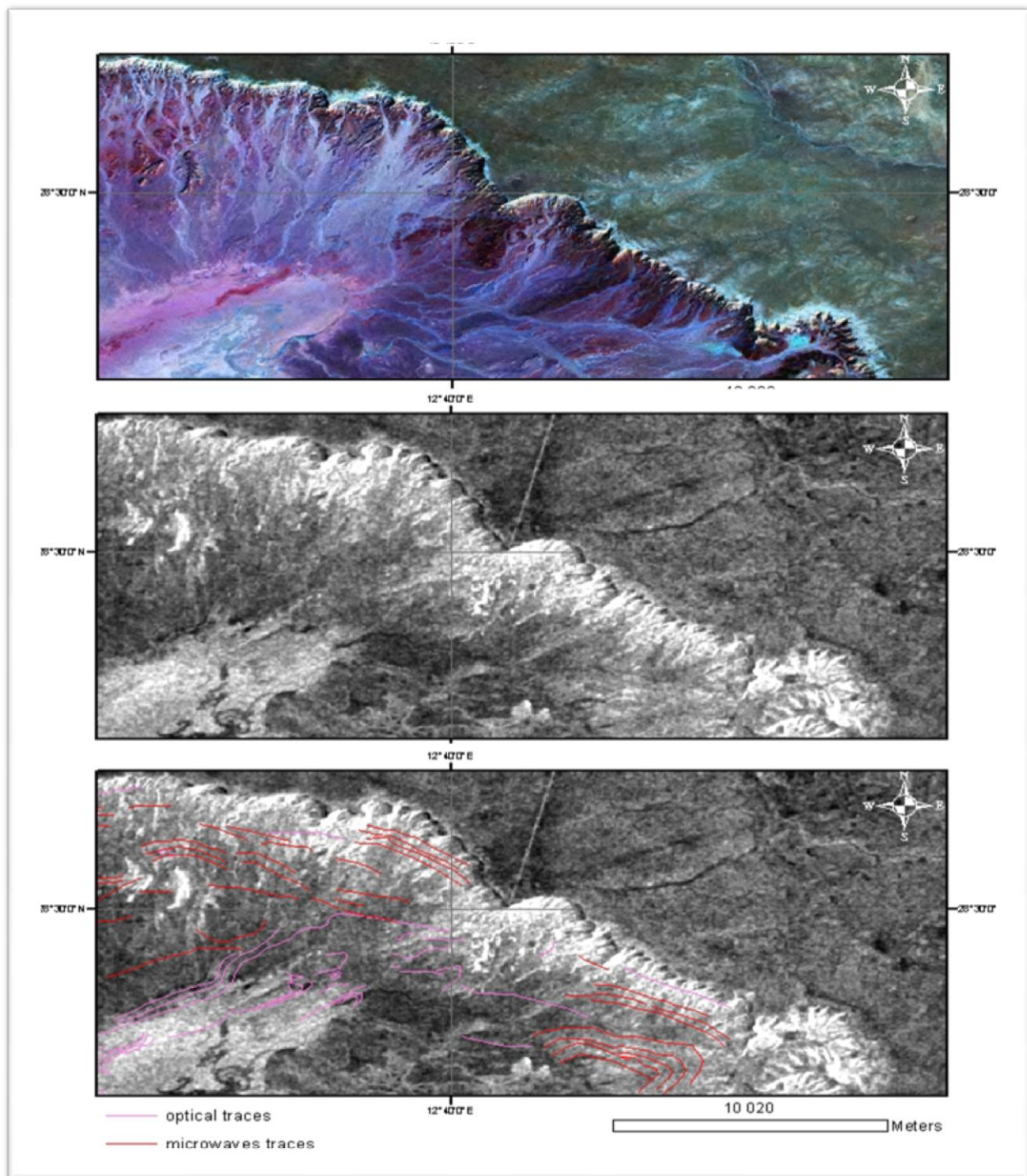


Figure 21: The SAR ERS image shows more layer traces in the Marar formation of Carboniferous age.

The Cenozoic faulting in the Al Hamra al Hamadah plateau is largely influenced by the tectonics affecting the Paleozoic oil bearing structures that are hidden by the late Cretaceous-Paleocene layers. The tectonic style is that of reactivation of the Paleozoic faults under effects of the NNE-trending regional tension.

Then the faults on the surface of the plateau would indicate location of the hidden Paleozoic faults in depth. A flat plateau, in arid environment, appears to be a very favourable environment for mapping of gentle folds, faults and tectonic sinkholes.

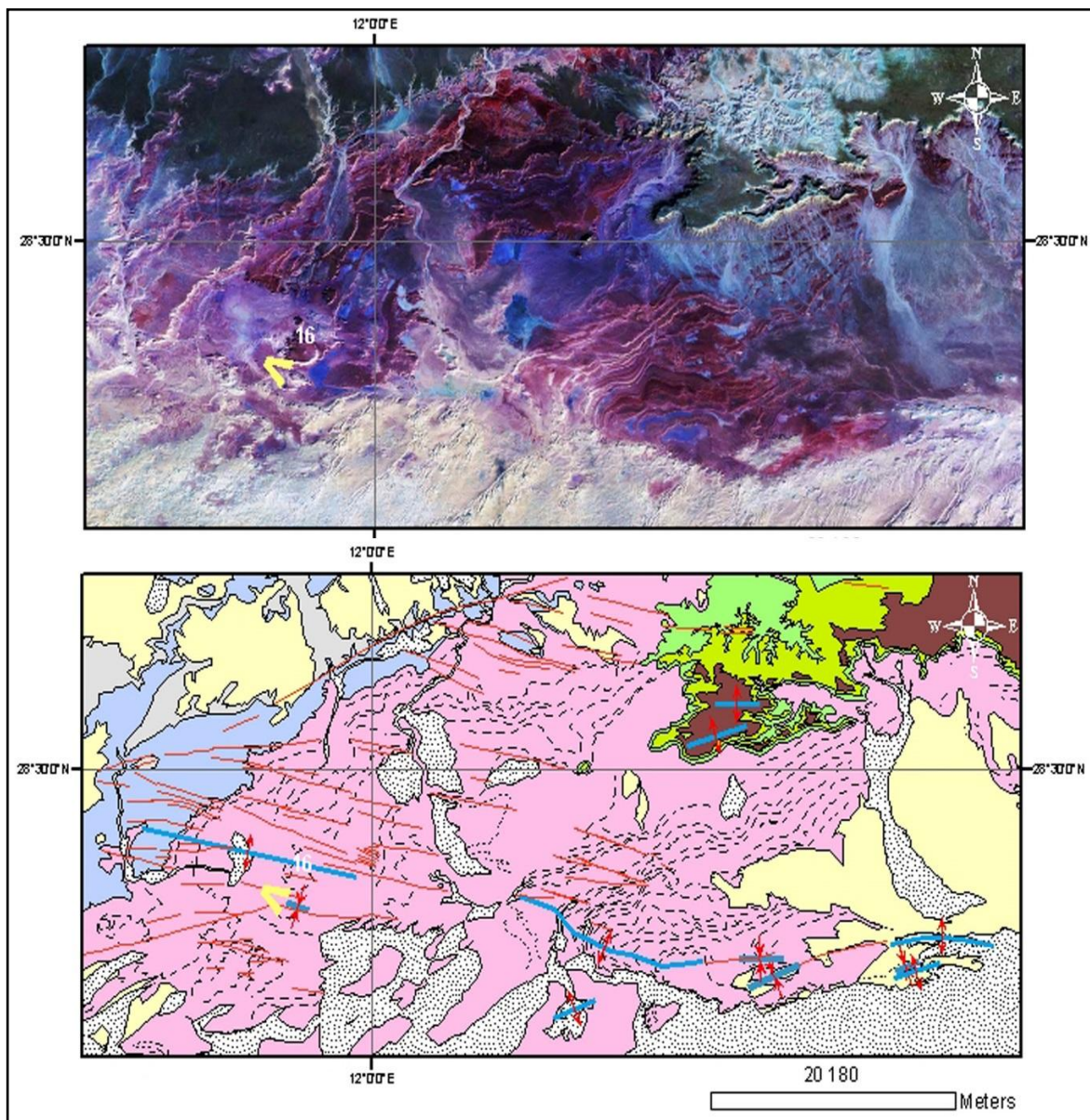


Figure 22: Western part of carboniferous outcrops, same legend as Figure 20. The GoogleEarthview n° 16 of Figure24. GoogleEarth views are located on the Landsat image.

Remote sensing is a fruitful approach in this study. The gentle anticlines for instance are undetectable in the field,

but computer assisted shadowing with a low elevation angle of illumination is the key processing for evidencing these features.

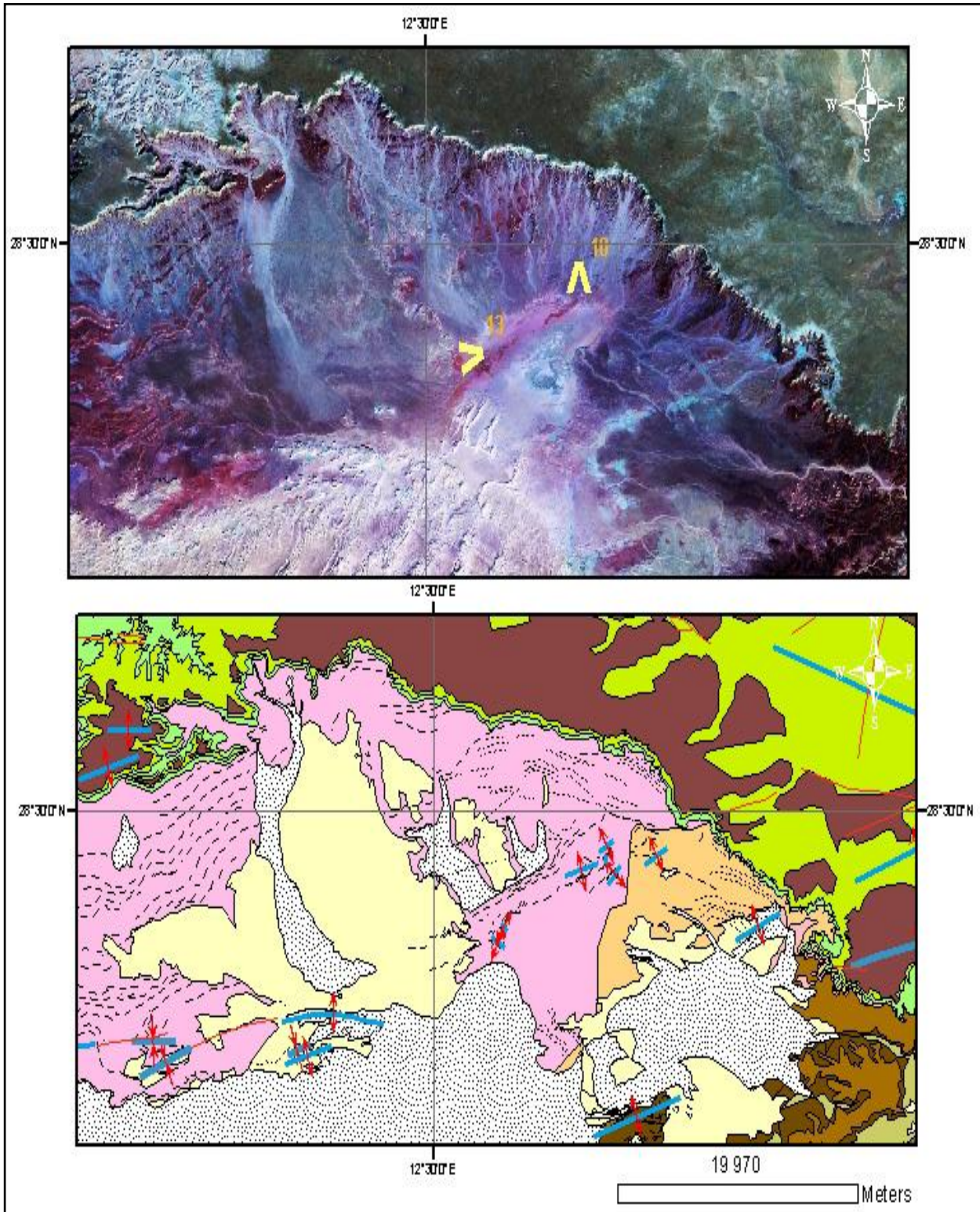


Figure 23: Eastern part of carboniferous outcrops, same legend as Figure 20. The GoogleEarth views n° 10 and 13 of Figure 24. GoogleEarth views are located on the Landsat image.

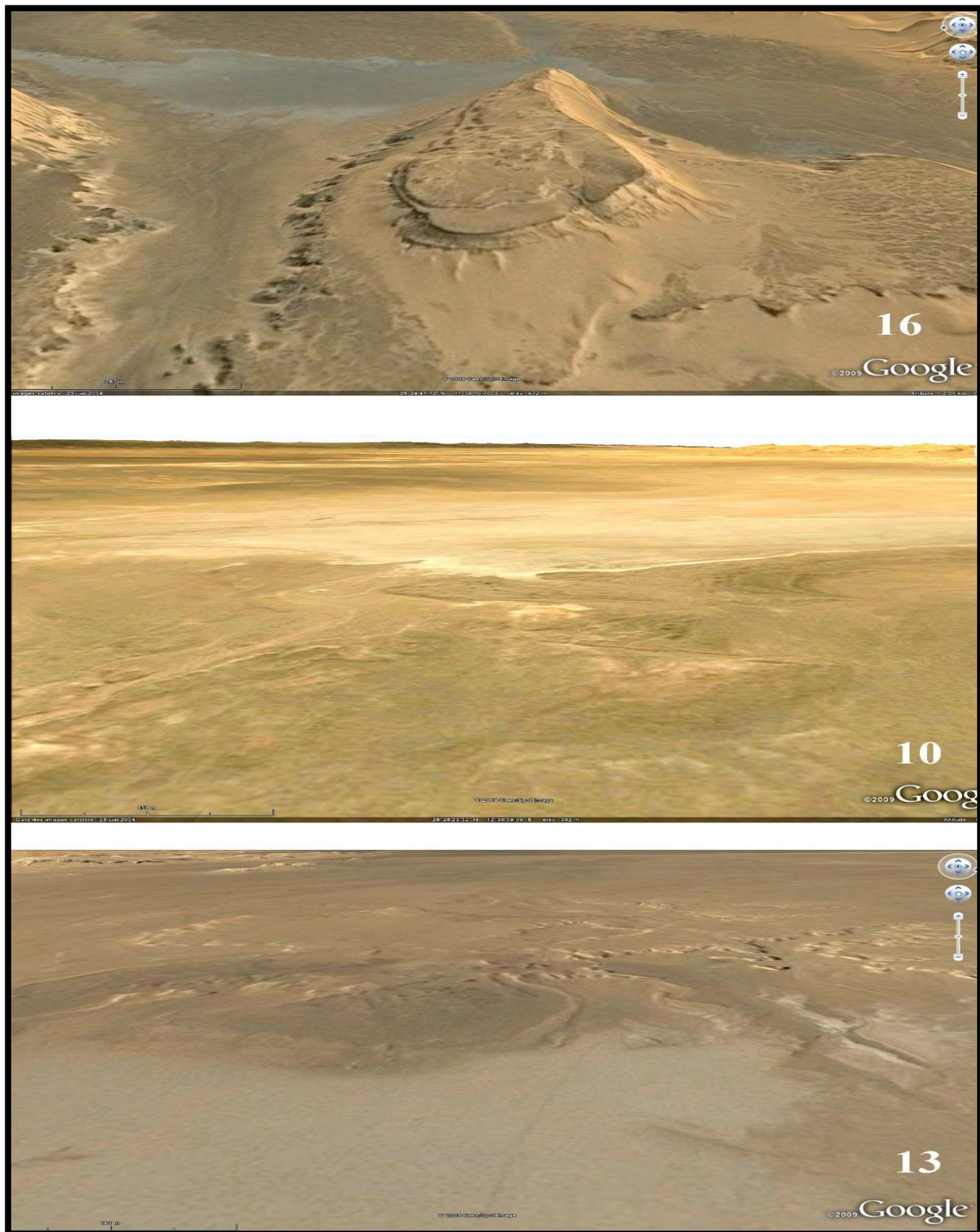


Figure 24: GoogleEarth views. Smaller scale folding affects the Marar formation near the axe zone of the larger anticline regional scale of trans-tensional deformation responsible for the uplift of the Qarqaf arch. This interpretation excludes the possibility to interpret the compression affecting the Devonian-Carboniferous layers as being related to a regional compressional Hercynian belt (Figure 25).

The tectonic model for interpreting this tectonics was suggested by (Glover et al., 2000), proposing that soft deposits are supposed to slide over uplifting basement inclined layers, at the end of their deposition. This interpretation implies that compressional deformation occurred only inside the displaced mass material sliding. It is then not contradictory with the tectonic model proposed at

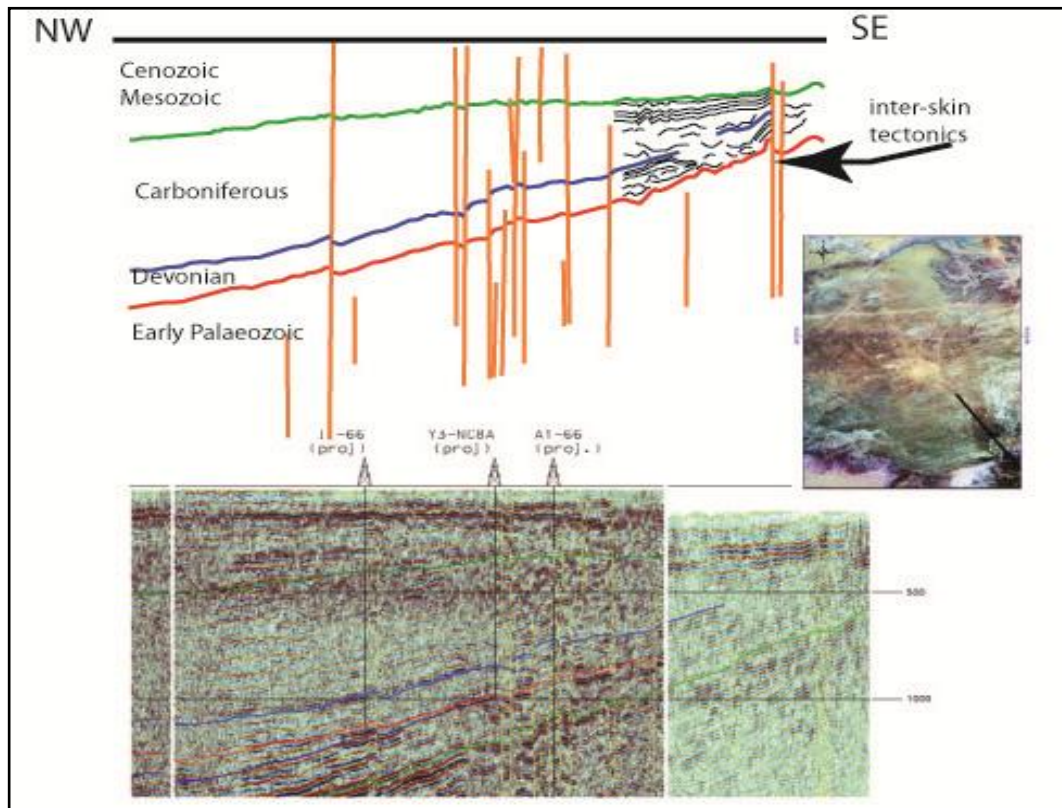


Figure 25: Seismic profile across the plateau, in the eastern induced prolongation of the Carboniferous layers. Location on the Landsat image. The interpretation evidences disharmonic interskin tectonics

7. Acknowledgements

I am thankful to Libyan Petroleum Institute Tripoli-Libya, for providing the data-base for this study. I would like also to express my sincere thanks and appreciation to the Prof. Jean Chorowicz, for his encouragement to publish this paper. Thanks also extended to the anonymous reviewers (Internal and External) for their fruitful suggested comments. Special thanks and gratitude go to my family for their patient and support to finish this paper.

8. Conclusions

- We have modified the new geological map and history of the studied area.
- The geological maps obtained with the method used represent the units one by one with each a shape-file, showing the geology in depth by scorching off the map. The final outcrop map is the result of the superimposed GIS layers.
- Our mapping has provided significant results, such as the evidencing of the downthrown Wadi Ash Shabiyat block, the description of the Bir Aishah gentle anticline, and sorting of the fracturing (More details : Benissa, M.A. and J. Chorowicz, 2016).
- This paper also shows the importance of up-dating the ancient geological maps using remote sensing. The Remote sensing analysis is an efficient tool for updating geological maps.
- The new mapping and the shadowing of DEMs has evidenced a series of gentle anticlines with axes trending NNE-SSW to NNW-SSE, affecting the late Cretaceous-

Paleocene plateau, which were previously all but one unknown.

- The analysis of hydrologic network anomalies has resulted into the mapping of a few lineaments and of part of the faults.
- The gentle anticlines for instance are undetectable in the field, but computer assisted shadowing with low elevation angle of illumination is the key processing for evidencing these features.
- According to our structural analysis, Al Qarqaf arch is a strike-slip fault zone, on the whole dextral, comprising N80°E dextral strike-slip faults and also coeval sinistral N110°E conjugate faults. The deformation started in the Cambrian (Benissa, M.A. and J. Chorowicz, 2016).
- The fractures were created in tensional environment, forming openings that were immediately filled by sedimentary dikes.
- In places, very local push-up compressions occurred along the strike-slip faults, forming some folds.
- The fracturing was dense at the beginning, but progressively the movements concentrated in few faults during the Cambrian to Silurian time.
- The compressional structures that exist in the area, are local particularities related to push-up relay zones along strike-slip faults, of drag fold related to normal faulting.
- No structures related to a Hercynian orogeny have been found. There no evidence of a major Hercynian compressional tectonic event during the Carboniferous.
- We infer that the whole Palaeozoic time interval in the region is marked by extension starting in the early Palaeozoic, forming a rift system, in which coeval graben depo-centres were linked by the transfer fault zone.

- This tectonics gave way to subsequent rift thermal evolution in continental environment, and finally the genesis of the Ghadamis and Murzuk basins throughout the Palaeozoic.
- This leads to a new concept about the tectonic style of the structures affecting the Palaeozoic series in Libya.
- The related structures, regional unconformity, faults and folds, which were participate the oil traps, should rather be regarded to result from this major and long duration phase of extension.
- The uplift of anticlines was of the order of 20m maximum.
- The analysis of hydrologic network anomalies has resulted into the mapping of a few lineaments and of part of the faults.
- In the southern part of the Ghadamis basin, a WNW-trending lineament, forming the northern boundary of a great number of faults striking the same, seems to mark the northern boundary of the densely fractured Al Qarqaf arch, which was a strike-slip transfer fault zone during the Palaeozoic time interval.
- To the east of Ghadamis basin, NNW-trending lineaments seem to represent the western boundary of the area subjected to faulting related to evolution of the Hon graben.
- Another major outcome of this study is that interpretation of the numerous sinkholes spread all over the area, in terms of tectonic openings such as tension fractures or pull-apart features, is consistent with the tectonic framework.
- A stable, long duration (late Eocene to Quaternary) regional tensional stress-field was oriented NNE-SSW. It is responsible for genesis of the tectonic sinkholes, faults, the Hon graben and volcanism.
- The volcanic venues in south-eastern part of the study area are related with the opening of tension fractures during the (Miocene?)-Pliocene-Quaternary time.
- The Cenozoic faulting in the Al Hamra al Hamadah plateau is largely influenced by the tectonics affecting the Palaeozoic oil bearing structures that are hidden by the late Cretaceous-Palaeocene layers. The tectonic style is that of reactivation of the Palaeozoic faults under effects of the NNE-trending regional tension. Then the faults on the surface of the plateau would indicate location of the hidden Palaeozoic faults in depth.
- We favour a hypothesis based on their rather Cenozoic age, which implies that concentration of low density oil material in depth, inside the Palaeozoic traps, and subsequent tendency to uplift, should have been transferred across the late Cretaceous-Paleocene sedimentary pile, and up to the surface.
- The oil and gas fields discovered in the Ghadamis basin occur, up to now, in pure structural traps or in complex combined structural-stratigraphic traps. The exploration of the basin may enter a new era. The study led to the good understanding of the geological structure setting with relationships of petroleum systems and the hydrocarbon charge appears to be present in most of the Ghadamis basin.
- Most of the exploratory wells have oil and gas shows. Several of the wells drilled in the first period of exploration are not conclusive as they are often ill-located and sometimes out of the structures.

- Integration of remote sensing data of different spatial and/or spectral characteristics and digital elevation models (DEM) can extremely effective in mapping morphologically-defined structures.
- The applications for the images returned by the first SPOT mission are land-use studies, mineral and hydrocarbon exploration.

References

- [1] AMMP, 1992. African magnetic map, ULIS Ltd, University of Leeds Industrial.
- [2] Barringer, A.R. 1970: Remote sensing techniques for mineral discovery. Commonwealth Mining and Metallurgical Congress, 5th, 1969. London: Institution of Mining and Metallurgy. v. 2. pp. 649-90.
- [3] Benissa, M.A. and J. Chorowicz, 2016: Remote sensing and field analysis of the Paleozoic structural style in NW Libya: The Qarqaf arch a Paleo-transfer fault zone between the Ghadamis and Murzuq basins. Journal of African Earth Science 123 (2016) 272-293.
- [4] Chorowicz J. & Deroin, J.P., 2003. La télédétection et la cartographie géomorphologique et géologique. Editions Gordon & Breach, collection Géosciences, 141 p.
- [5] Chorowicz, J., Collet, B., Bonavia, F. & Tesfaye, K., 1994. NW-to NNW extension direction in the Ethiopian Rift deduced from the orientation of structures and fault slip analysis. Geological Society of America Bulletin, 105, 1560-1570.
- [6] Chorowicz, J., Le Fournier, J., Le Mut, C., Richert, J.P., Spy-Anderson, F.L. & Tiercelin, J.J. 1983. Observation par télédétection et au sol de mouvements décrochants NW-SE dextres dans le secteur transformant Tanganyika-Rukwa-Malawi du Rift Est-Africain. C. R. Acad. Sc. Paris, 296, sér.II, 997-1002.
- [7] Glover et al., 2000. The onset and Association of CMEs with Sigmoidal Active Regions: geophysical research letters, vol. 27, no. 14, pages 2161-2164, July 15, 2000, Mullard Space Science Laboratory, Dorking, Surrey, UK.
- [8] Jeffrey, D., Phillips, Richard, W., Saltus, Richards, L., Reynolds, 1998. Source of magnetic anomalies over a sedimentary basin: preliminary results from the coasta plain of the Arctic National wildlife, Alaska, in Geologic applications of gravity and magnetic: case histories, (R. I. Gibson and P. S. Millegan, Editors), AAPG studies in geology 43, SEG Geophysical reference series, no 8.
- [9] Jones, V. T., III, M. D. Matthews, and D. M. Richers (1999), Light hydrocarbons for petroleum and gas prospecting, in Geochemical Remote Sensing of the Subsurface, Handbook of Exploration Geochemistry, vol. 7, edited by G. J. S. Govett and M. Hale, Elsevier, New York.
- [10] Z.Ghanmi¹²M.Rouabhia¹²O.Othmane¹²P.A.Deschaux, 1987: Effects of metal ions on cyprinid fish immune response: *In vitro* effects of Zn²⁺ and Mn²⁺ on the mitogenic response of carp pronephros lymphocytes, Ecotoxicology and Environmental Safety, Volume 17, Issue 2, April 1989, Pages 183-189.